Design Thickness Requirements for Hollow Structural Sections

by

Muzomkhulu Ncube

Submitted in partial fulfilment of the requirements
for the degree of Master of Applied Science

at

Dalhousie University
Halifax, Nova Scotia
July 2024

TABLE OF CONTENTS

LIST OF TABLES

LIST OF FIGURES

ABSTRACT

The Canadian design wall thickness requirements, t, for ASTM A500 hollow structural section (HSS) members is set at 0.90 times the nominal thickness, t_{nom}. The American Institute of Steel Construction (AISC) specifies the same as $0.93t_{nom}$. This discrepancy gives rise to questions as to the economic sufficiency of the Canadian standard set by the Canadian Standards Association (CSA) and the Canadian Institute of Steel Construction (CISC). Dimensional data obtained from quality control records, field measurements, and the literature representing modern manufacturing practices for ASTM A500 HSS is compiled and used to compute basic statistics (i.e., means and coefficients of variation of actual-to-predicted cross-sectional area, moment of inertia, radius of gyration, elastic and plastic moduli). The forgoing statistics, combined with ASTM A500 HSS material property statistics, are used collectively to derive professional factors for modern CSA S16 design formulae. A reliability analysis is carried out to assess the level of safety obtained when using the currently prescribed design wall thicknesses and alternatives for ASTM A500 members in accordance with CSA S16.

Keywords: Hollow structural sections, design wall thickness, reliability.

LIST OF ABBREVIATIONS AND SYMBOLS

AISC	=	American Institute of Steel Construction
ASCE	=	American Society of Civil Engineers
ASTM	=	American Society for Testing and Materials
CISC	=	Canadian Institute of Steel Construction
CHS	=	Circular Hollow Section
COV	=	Coefficient of Variation
CSA	=	Canadian Standards Association
ERW	=	Electric Resistance Welded
FORM	=	First Order Reliability Method
HSS	=	Hollow Structural Section
LRFD	=	Load and Resistance Factor Design
RHS	=	Rectangular Hollow Section
SABS	=	South African Bureau of Standards
STI	=	Steel Tube Institute
A_g	=	gross cross-sectional area
A_{net}	=	net cross-sectional area
C_r	=	axial compressive resistance of steel above neutral axis (in CSA S16:24 Cl 13.3.1.1)
D	=	dead load
E	=	modulus of elasticity of steel
F_y	=	yield stress
I	=	moment of inertia
KL	=	effective length
L	=	live load; length of member
M_n	=	nominal flexural strength
R	=	resistance
R_n	=	nominal resistance
S_i	=	nominal load effect
V	=	coefficient of variation

V_d	=	coefficient of variation for discretization factor
V_G	=	coefficient of variation for geometric properties
V_M	=	coefficient of variation for material properties
V_P	=	coefficient of variation for professional factor
V_R	=	coefficient of variation for resistance
V_s	=	coefficient of variation for load effect
V_t	=	coefficient of variation for wall thickness
Z	=	plastic modulus
b	=	outside width of RHS
b_i	=	inner width of RHS (= $b - 2t$)
d	=	outside diameter of CHS
d_i	=	inner diameter of CHS
h	=	depth of RHS
i	=	source
k_a	=	axial stiffness
k_b	=	bending stiffness
n	=	number of data points
n	=	column curve parameter
r	=	radius of gyration
r_i	=	inside corner radius of RHS
r_o	=	outside corner radius of RHS
t	=	design wall thickness
t_{nom}	=	nominal wall thickness
α_i	=	load effect factor
β	=	reliability index
δ	=	bias coefficient
δ_d	=	bias coefficient for discretization factor
δ_G	=	bias coefficient for geometric properties
δ_M	=	bias coefficient for material properties
δ_P	=	bias coefficient for professional factor
δ_t	=	actual-to-nominal thickness ratio
λ	=	non-dimensional slenderness parameter
ϕ	=	resistance factor

ACKNOWLEDGMENTS

I would like to express my deepest gratitude to those who have supported me throughout the journey of completing this research thesis.

First and foremost, I am immensely grateful to my beloved wife, Laura, for her unwavering support, patience, and understanding. Her encouragement and sacrifices have been the cornerstone of my success. Her belief in me kept me going even during the most challenging times.

I would also like to extend my sincere appreciation to my research supervisor, Dr. Kyle Tousignant, for his invaluable guidance, insightful advice, and continuous encouragement. His expertise and dedication have significantly contributed to the quality and depth of this research. I am truly fortunate to have had the opportunity to work under his mentorship.

Special thanks are due to the Southern African Students Education Project at Dalhousie University, whose generous financial support made my studies and this research possible. Their commitment to fostering academic excellence is commendable, and I am deeply thankful for their trust in my capabilities.

Finally, I would like to thank my family, friends, and colleagues for their support and understanding throughout this journey. Their encouragement has been a source of strength and motivation.

Soli Deo Gloria.

Chapter 1: INTRODUCTION

1.1. HSS MANUFACTURING STANDARDS

The principal options for Hollow Structural Sections (HSS) in Canada are products manufactured to Canadian Standards Association (CSA) Standard G40.20 in Class C or Class H (CSA 2018) from steel meeting the requirements of the "CSA G40.21" material standard (CSA 2018) or American Society of Testing and Materials (ASTM) A500/A500M grade C (ASTM 2023). The relative availability of these alternatives varies around the country, as described in Table 6-8 of the Canadian Institute of Steel Construction (CISC) Handbook of Steel Construction (CISC 2021).

One further HSS product, ASTM A1085 (ASTM 2015), is now heavily promoted in North America as a desirable substitute for ASTM A500. A1085 is directly equivalent to the G40 Class C (CSA 2018) product except that the specified minimum yield strength (F_y) is 345 MPa and there is a minimum Charpy impact toughness provided (whereas a Charpy notch toughness rating needs to be called up with G40 Class C by an additional toughness Category number). Section properties for ASTM A1085 are identical to those for CSA G40. Consequently, if ASTM A1085 is ordered in Canada one is directed to substitute with CSA G40 Class C.

1.1.1. CSA G40.20/G40.21

CSA G40 HSS is produced as cold-formed Circular Hollow Sections (CHS) and Rectangular Hollow Sections (RHS) from round by an electric resistance welding (ERW) process, to a single grade of 350W with a specified minimum yield strength (F_y) of 350 MPa. A tolerance of -5% is permitted on wall thickness, with a further tolerance on mass (and hence effectively cross-sectional area) of -3.5%. These stringent tolerances ensure structural reliability comparable to competing hot-formed open sections, hence a design wall thickness (t) equal to the nominal thickness (t_{nom}) is applied.

Section properties are provided in the CISC Handbook (CISC 2021), where the outside corner radius of RHS (r_o) is taken to be $2t$ and the inside corner radius (r_i) is taken to be equal to the design wall thickness, t. The cold-formed HSS end product (Class C) can be heat-treated to form an alternative Class H product by heating to 450° C or higher, followed by cooling in air. Class H enables a higher compressive resistance for HSS columns.

1.1.2. ASTM A500

ASTM A500 (ASTM 2023) HSS is cold-formed from round by ERW in Canada, to CHS and RHS shapes. In theory, grades B and C are available for each of CHS and RHS, but the product is now routinely dual-certified to both grades B and C and hence only the higher grade (C) need be specified. This is reflected in the CISC Handbook Part 4, where compressive resistance tables are provided for unfilled HSS for only ASTM A500 grade C. The specified minimum yield strength, F_y, of RHS grade C is 345 MPa, and until 2021, F_y was 317 MPa for CHS grade C. In 2021, the specified minimum yield strength, F_y, for ASTM A500 Grades B and C HSS in Table 2 of ASTM A500 (2023) were harmonized to 315 MPa and 345 MPa, respectively (reflecting an 8-10% increase for round HSS products).

A500 (ASTM 2023) permits a tolerance of -10% on wall thickness, with no tolerance specifications on mass, weight, or cross-sectional area, resulting in HSS being produced routinely undersize since manufacturers interpret tolerances as allowances. CISC (2021) hence stipulates a design wall thickness of $t = 0.90t_{nom}$ for structural design with A500 in Canada. This design wall thickness is incorporated already in the A500 section properties provided in the CISC Handbook, along with an assumed outside corner radius of $2t$ for RHS (CISC 2021).

When A500 HSS members are used as seismic braces, CSA S16:24 requires that nominal section properties be used for determining the probable resistance. For members available in both A500 and CSA G40 grades, the table of section properties for G40.21 may be used for design purposes.

1.1.3. Other HSS Manufacturing Standards

The British Standards Institution also provides a set of guideline documents for manufacturing and design of HSS. These are commonly referred to as Euronorm (EN) standards for their use across the European Union and have also found widespread acceptance in Commonwealth nations. EN 10210 (BS 2006) describes the technical requirements for Hot Finished HSS, while EN 10219 (BS 2006) describes those of cold formed welded HSS.

EN standards provide yield strength values of 355 MPa for sections of nominal thickness less than 16mm and 345MPa for sections of thickness greater than 16mm. A wall thickness tolerance of -10% is stipulated for EN 10210 sections. The same tolerance is applicable to EN 10219 sections of nominal thicknesses of 5mm or less, and a -0.5 mm tolerance limit is set for sections with thickness greater than 5mm. For both types of HSS, a mass or area tolerance of -6% is stipulated.

SANS 657-1 (SABS 2011) is the South African Bureau of Standards (SABS)' manufacturing standards for HSS steel intended for use in non-pressure purposes. Grade 355WA sections are produced with a stipulated minimum yield strength of 355MPa. A mass, and therefore cross-sectional area, tolerance of -10% is stated for

both steel grades. Wall thickness tolerance varies from -9% to -6% depending on the nominal thickness of the section.

Another common standard for the manufacture of cold-formed HSS steel is the AS/NZS 1163 (Standards Australia 2016) which is used in Australia and New Zealand. Sections are produced in two classes, C350L0 and C450L0 with a stipulated minimum yield strength of 350 MPa and 450 MPa respectively. A mass or area tolerance of -4% and a wall thickness tolerance of -10% for all sections is specified. Table 1-1 summarises these common international guidelines for the manufacture of HSS steel.

Table 1-1: Common international standards for HSS production and tolerance limits

Specification	Grade	F_y (MPa)	F_u (MPa)	Wall Thickness Tolerance	Mass or Area Tol-erance
ASTM A500	C - CHS	315	427	-10%	-
	C- RHS	345	427	-10%	-
CSA G40.20/G40.21	350W	350	450	-5%	-3.5%
EN 10219	S355J2H	355 for $t \leq 16$ mm; 345 for $16 < t \leq 45$mm	470 for $3 < t \leq 40$mm	-10% for $t \leq 5$ mm; -0.5 mm for $t > 5$ mm & for $D \leq 406.4$ mm	-6%
AS/NZ 1163	C350L0	350	430	-10% for $D \leq 406.4$ mm	-4%
	C450L0	450	500		
SANS 657-1	355WA	355	450	-9% for 3mm $\leq t \leq$ 4mm; -7.5% for $4 < t \leq 5$ mm; -6.5% for $5 < t \leq 6$ mm; -6% for $t > 5$ mm	-10%

1.1.4. SUMMARY

Having discussed broadly the standards governing structural steel manufacturing around the world, with particular emphasis on North American standards for HSS sections, it is incumbent upon the thesis author to highlight that the long-term objective of this research study is to review and if necessary, propose a modification to the design thickness requirements for ASTM A500 HSS in CSA S16:24.

1.2. RESEARCH BACKGROUND

1.2.1. A500 HSS DESIGN THICKNESS REQUIREMENTS

The ASTM A500 (2023) production standard permits a deviation in wall thickness of -10%, with no tolerance on mass, weight, or cross-sectional area. For these sections, CISC stipulates that a design wall thickness of $t = 0.90t_{nom}$ must be used. This design wall thickness is already incorporated into the section

properties in CISC's Handbook (2021). On the other hand, in the United States (US), AISC (2016, 2017) stipulates a larger design wall thickness of $t = 0.93t_{nom}$ for ASTM A500 HSS.

This so-called "ASTM A500 design thickness issue", whereby $t = 0.90t_{nom}$ in Canada but $t = 0.93t_{nom}$ in the US has been long-debated within CSA and the CISC, and has a sizeable (and, likely, undue) economic implication. Tables 1-2 and 1-3 illustrate how these seemingly small changes in t affect the compressive and flexural resistance (and, hence, the economy) of HSS members.

The variation in flexural resistance is further compounded by the influence of the design wall thickness considered on the classification of the section according to the limits provided by Table 2 of CSA S16:24. Some sections may be on the threshold of two classes, for example Class 2 and Class 3, when the design thickness is taken at different values. The flexural resistance of a section (and consequently, its economy) can be greatly improved as the design thickness is increased resulting in the section classification varying. This is the case for the two latter sections in Table 1-3 below, which show a big reduction in strength when the design thickness is taken as the lower considered value of $0.90t_{nom}$.

Table 1-2: Compressive resistance (in kN) of selected ASTM A500 HSS assuming $t = 0.90$, 0.93, and $1.00t_{nom}$

Designation	$t/t_{nom} = 1.00$	$t/t_{nom} = 0.93$	$t/t_{nom} = 0.90$
HSS 203×203×4.8	470	400 (-15%)	380 (-19%)
HSS 864×254×19	4850	4270 (-12%)	4040 (-17%)
HSS 508×6.4	1250	1130 (-10%)	1080 (-14%)

Note: calculated according to CSA S16 with $F_y = 345$ MPa and $KL/r = 100$.

Table 1-3: Flexural resistance (in kNm) of selected ASTM A500 HSS assuming $t = 0.90$, 0.93, and $1.00t_{nom}$

Designation	$t/t_{nom} = 1.00$	$t/t_{nom} = 0.93$	$t/t_{nom} = 0.90$
HSS 508×508×13	1230	1000 (-19%)	950 (-23%)
HSS 457×9.5	590	550 (-7%)	410 (-31%)
HSS 610×13	1400	1310 (-6%)	980 (-30%)

Note: calculated according to CSA S16 with $F_y = 345$ MPa.

1.2.2. Research Scope and Objectives

What is clearly needed, as a long-term objective, is to review and/or modify the design thickness requirements for ASTM A500 HSS in CSA S16, as the current approach (taking the design thickness as 0.9

times the nominal thickness) may have undue economic implications – particularly for jumbo HSS. This long-term objective defines the general scope of this research.

The primary objectives of the research are to:

1. Obtain/measure dimensional data (from quality control records, field measurements, and/or the literature) that represent modern manufacturing practice for ASTM A500 HSS;
2. Using the above, compute basic geometrical property statistics i.e., means and coefficients of variation (COVs) of actual-to-predicted cross-sectional area, moment of inertia, etc;
3. Amalgamate the forgoing data with recently obtained HSS material property and professional factor (i.e., actual-to-predicted strength) statistics for modern CSA S16:24 design formulae [from Liu (2016) and Schmidt and Bartlett (2002), respectively]; and
4. Carry out a reliability study in accordance with CSA S408-11 (2011) on the implications of using t = 0.90, 0.93, and $1.00t_{nom}$ for the ASTM A500 design wall thickness in Canada.

The scope of this research covers a review of the design thickness requirements set out by CSA S16 on A500 HSS members. Compression members, tension members, and laterally restrained beam bending of both CHS and RHS sections is considered.

Chapter 1 presents a brief background and description of the research project, specifying the challenge leading to the project statement, followed by a breakdown of the project scope and objectives.

Chapter 2 discusses the methodology adopted in meeting the research objectives. The scope and nature of the dimensional data for A500 HSS members is discussed herein, along with a specific discussion of the method by which the sampled dimensions were obtained in line with current standards set forth by literature.

Chapter 3 discusses the details of the dimensional data collected, and the statistical parameters resulting from the analysis of this sampled data. The material properties statistical parameters relevant to this research are also discussed, having been sourced from relevant literature.

Chapter 4 discusses the First Order-Reliability Method analysis used in this study. An extensive discussion of the history of reliability analysis and its application in Canadian standards calibration is followed by a mathematical discourse of the development of the FORM analysis.

Chapter 5 covers the resistance statistics developed from the material and geometric statistical parameters, and how these resistance statistics differ with the loading conditions considered, i.e., compression, tension and bending.

Chapter 6 outlines the results of the FORM analysis in each of the three loading conditions considered. An extensive discussion of the results and how they vary depending on section profiles and loading conditions is given.

Chapter 7 discusses conclusions drawn from the results of the study when juxtaposed with the research objectives. A summary of the research work undertaken is given, followed by conclusions drawn and finally recommendations for future research work in support of and motivated by this current body of work.

Chapter 2: METHODOLOGY

2.1. DIMENSIONAL TOLERANCES FOR HSS MANUFACTURED TO ASTM A500

The document "Methods to Check Dimensional Tolerances on Hollow Structural Sections" (STI 2021), updated in August 2021, was published by the Steel Tube Institute (STI) as a guide for obtaining HSS dimensions. Within this guide, methods for checking dimensional tolerances as stipulated in Section 11 of ASTM A500-20 (ASTM 2020) (see Section 2.2 of this thesis) are discussed in detail. These methods, discussed below, are also applicable to checking tolerances for HSS made to ASTM A1085 (ASTM 2015), CSA G40.20/G40.21 (CSA 2018) and other HSS material specifications.

2.1.1. OUTSIDE DIMENSIONS (ROUND HSS)

According to Section 11.1 of ASTM (2020), the outside diameter of a round tube shall not vary more than ±0.5%, rounded to the nearest 0.005 in. [0.1 mm] from the specified outside diameter for specified outside diameters 1.900 in. [48mm], and smaller, and ±0.75%, rounded to the nearest 0.005 in. [0.1 mm], from the specified outside diameter for specified outside diameters 2.00 in. [50 mm] and larger. The outside diameter measurements shall be made at positions at least 2 in. [5 cm] from the ends of the tubing.

According to the STI Guide (STI 2021), to perform this measurement, one requires outside micrometers of a suitable size to check the round HSS.

The method is spelled out as follows (STI 2021):

1. Measure at a position at least 2 inches from either end of the HSS;
2. Outside diameter measurements should be made at a point 90 degrees to the weld line (direction a-a, Fig. 2-1) and at points on either side of the weld line (directions b-b and c-c).
3. Outside diameter measurements are not taken directly on the weld line.

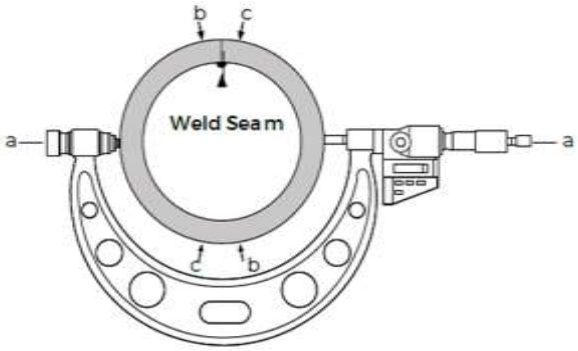

Figure 2-1: Procedure for measuring outside diameter of round HSS (STI 2021)

2.1.2. OUTSIDE DIMENSIONS (SQUARE AND RECTANGULAR HSS)

According to Section 11.1 of ASTM (2020), the outside dimensions measured across the flats shall not vary from the specified outside dimensions by more than the applicable amount given in Table 2-1.

Table 2-1:Allowable variation in outside dimensions

Specified Outside Large Flat Dimension, in. [mm]	Permissible Variations Over and Under Specified Outside Flat Dimensions, in. [mm]
2.5 [65] or under	0.020 [0.5]
Over 2.5 to 3.5 [65 to 90], incl.	0.025 [0.6]
Over 3.5 to 5.5 [90 to 140], incl.	0.030 [0.8]
Over 5.5 [140]	0.01 times large flat dimension

The permissible variations include allowances for convexity and concavity. For rectangular tubing having a ratio of outside large to small flat dimension less than 1.5 and for square tubing, the permissible variations in small flat dimension shall be identical to the permissible variations in large flat dimensions given in Table 2-1 above. For rectangular tubing having a ratio of outside large to small flat dimension in the range of 1.5 to 3.0 inclusive, the permissible variations in small flat dimension shall be 1.5 times the permissible variation in large flat dimension. For rectangular tubing having a ratio of outside large to small flat dimension greater than 3.0, the permissible variations in small flat dimension shall be 2.0 times the permissible variation in large flat dimension.

According to the STI Guide, outside micrometers of a suitable size are required to perform the measurement of the outside dimensions of square or rectangular HSS. Calipers or measuring tapes are considered unsuitable for measurement purposes.

The method of measurement is specified as follows:

1. Measure at a position at least 2 inches (50 mm) from either end of the HSS.

2. Each side of the tube requires measurements across the flats to ascertain not only the size but convexity or concavity as well. These measurements should be made near the start of the outside corner radii (directions a-a, c-c, d-d and f-f, Fig. 2-2) and near the center of the flats (directions b-b and e-e, Fig 2-2). The measurement across the flat containing the weld should be made at a point on either side of the weld line.
3. Measurements shall not be taken directly on the weld line.

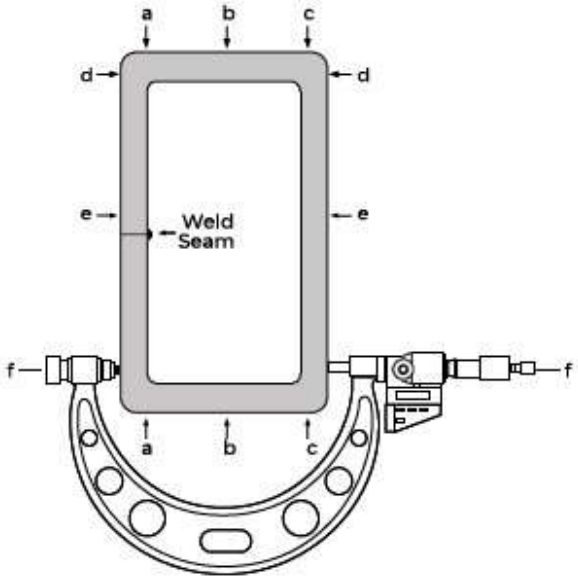

Figure 2-2: Procedure for measuring outside dimensions of square and rectangular HSS (STI 2021)

2.1.3. WALL THICKNESS (CIRCULAR HSS)

According to Section 11.1 of ASTM, the minimum wall thickness excluding the weld seam of welded tubing shall be not more than 10% less than the specified wall thickness. The maximum wall thickness, excluding the weld seam of welded tubing, shall be not more than 10% greater than the specified wall thickness. If the welded tubing is supplied with the inside flash removed, then the weld seam shall be included in the wall thickness measurement. The thickness limitations do not apply for the wall thickness measurement directly on the weld seam if the inside flash has not been removed.

An outside micrometer with a spherical anvil in the 0-1 in. range is required to perform the measurement of the wall thickness, according to the STI Guide. The measurement can be measured on any area of the HSS except in the area of the weld seam to avoid inaccurate measurements due to the presence of an inside weld bead in this area.

2.1.4. WALL THICKNESS (RECTANGULAR HSS)

For square and rectangular tubing, the wall thickness requirements are the same as those specified for round tubing, according to Section 11.1 of ASTM. These shall apply only to the centers of the flats of the tubing.

According to the STI Guide, outside micrometers with a flat anvil in the 0-1 in. range are required to perform the measurement of the wall thickness. Measurements shall be taken in the center of a flat. Due to thickening caused by the manufacturing process and the presence of an inside weld bead, measurements shall not be taken around the weld seam.

2.1.5. CORNER RADIUS (SQUARE AND RECTANGULAR HSS)

Section 11.6 of ASTM specifies that the radius of each outside corner of the section shall not exceed three times the specified wall thickness.

The STI Guide requires radius gauges to be used to perform the measurement of corner radii. The method of measurement is specified as follows:

1. Multiply the specified wall thickness of the HSS to be checked by three. This is the maximum outside corner radius allowed.
2. Select the radius gauge corresponding to the maximum outside corner radius allowed.
3. Apply the gauge to each corner of the tubing and note the fit.
4. If the gauge is too big or too small, remeasure with the next gauge size up or down until a good fit is obtained, which conforms to the profile of the HSS corner.
5. Note the gauge size and ascertain that each of the four corners is within the specification tolerance.

The foregoing measurements do not purport to account for length and straightness variations, variations in the squareness of sides (which can affect the cross-sectional properties), or twist. These variations are outside of the scope of the current study.

2.2. RELEVANT RESEARCH

Foley (2011) provides a report prepared for the AISC HSS Committee titled “Characterising Dimensional Variability in HSS Members.” The broad objective of the report was to inform the Committee regarding design related cross-sectional parameters and the potential for cracking in the corners of HSS members. Of interest to this thesis are the two primary objectives of the research which aim to characterise the variation in HSS wall thickness from a representative sample of HSS members provided by producers and to characterise the variability in wall thickness to address the suitability of the inherent $0.93t_{nom}$ limit on cross sectional thickness present in ASTM (AISC 2016).

In the research for the report, sixteen measurements were taken at each end of the specimen. Four measurements were taken from the centers of the flats, eight from the edges of the flats just before the corners, and four at the centers of the corners. The report specifies that these measurements were taken 1 in. from the end of each specimen, using a standard point micrometer. It is noteworthy at this point that the measurement procedure utilised in Foley (2011) is different from that recommended by STI (2021) and discussed in Section 2.2.3 of this thesis. STI (2021) recommends measurements be taken 2 in. away from the specimen edge, and that only four measurements are necessary, taken from the centers of the flats.

Foley (2011) concludes from the study that the mean HSS wall thickness from the sections received ranged from $0.954t_{nom}$ to $0.978t_{nom}$, and that a two standard deviation cushion implied a lower bound of $0.879t_{nom}$.

Schmidt and Bartlett (2002a,b) conducted research titled "Review of Resistance Factor for Steel." The research produced two papers, with the first covering "Data Collection" and the second "Resistance Distributions and Resistance Factor Calibration." The overall objective of the study was to review the applicability of the 0.90 resistance factor to steel production standards in 2000.

In the former paper, the resistance factor of 0.90 crafted by the study conducted by Kennedy and Gad Aly (1980) is noted to have remained unchanged for over 40 years. On the other hand, significant changes have been introduced to the production of structural steel which may influence the geometric properties of steel members. These changes include the increased use of recycled materials rather than raw materials in steel production, changes in material grades and therefore yield strength values and improved quality control. A manufacturing standard change specific to HSS steel is also highlighted. The minimum allowable wall thickness of CSA G40.20 sections has increased from $0.9t_{nom}$ to $0.95t_{nom}$.

Dimensional data were collected from quality control records and from relevant literature records. These were used to compute geometric bias coefficients and coefficients of variation for the various steel shapes. For HSS shapes, wall thickness measurements were taken in accordance with CSA G40.20 (CSA 1998), which requires measurements to be taken from the center of a flat that does not have a seam or weld. This is quite similar to the STI (2021) recommendations for taking wall thickness measurements of HSS.

For HSS, the variation in wall thickness was found to be small, with coefficients of variation of the order of 1%. Schmidt and Bartlett (2002a) highlight two possible reasons for this. The first is the stringent tolerance limit for wall thickness imposed by the CSA. The second argument is that producers seek to maximise financial returns by making the lightest product possible that consistently meets the CSA tolerance standards. The same literature source highlights an informal statement by a steel producer to the effect that they intentionally order raw material in the form of hot rolled coil with a thickness that is slightly below the minimum tolerance because the forming process increases the thickness to acceptable levels. The impact of this is noted in the distribution of the wall thickness measurements for this same producer which are never greater than 1. It is of course notable and concerning that manufacturers consider tolerance parameters set by manufacturing standards such as CSA G40.20/G40.21 as the target thickness for production rather than targeting the nominal thickness. By the same

principle, the less stringent tolerance values of ASTM A500 would probably result in a reduced bias coefficient and/or an increased coefficient of variation, which further reinforces the need for the objectives of this thesis.

Chapter 3: MATERIAL AND GEOMETRIC PROPERTIES

3.1. SCOPE OF DATA COLLECTION

In this study, dimensional data representing modern manufacturing practices for ASTM A500 HSS were obtained from producer quality control (QC) records and the literature. Table 3-1 summarizes the scope of the data collected, where i = source and n = number of independent measurements.

Table 3-1: Scope of data collected

Source, i	Description of data	n	Geometric Range (mm)		
			b or h	D	t
AISC (2011)	RHS wall thicknesses	896	76.2-304.8	-	4.78-15.88
Producer A	RHS wall thicknesses	3057	-	-	3.18-25.4
	CHS wall thicknesses	325	-	-	4.78-15.88
	RHS outside dimensions	5040	50.8-863.6	-	-
	CHS outside dimensions	456	-	114.3-609.6	-
Producer B	RHS wall thicknesses	4542	50.8-304.8	-	3.18-15.88
	CHS wall thicknesses	1013	-	42.2-406.8	3.18-15.88

For the current study, wall thickness data for ASTM A500 RHS and CHS was obtained from the AISC (2011), and from QC records for two of the largest conglomerates in North America: Producer A (in Table 3-1) has historically rolled over 1.05 million tons of HSS annually (Zekelman Industries, 2023), whereas Producer B generates an annual structural steel output of 25 million tons (Nucor Corporation, 2023). Combined, this data set includes n = 9833 independent HSS wall thickness measurements (the largest in any one study) from two North American steel corporations owning a combined seven tube producers across 25 different production facilities. This accounts for at least 85% of the market share of HSS products used in North America at the time the data was collected for this study.

3.2. WALL THICKNESS

In the study by Kennedy and Gad Aly (1980), 302 wall thickness measurements for CSA G40.20/G40.21 (2013) RHS and CHS were summarized, in which the average measured-to-nominal thickness (δ_t, i.e., the bias factor for t), was 0.975 with a corresponding coefficient of variation (COV), $V_t = 0.025$. Schmidt and Bartlett (2002a) summarized 7764 HSS wall thickness measurements for CSA G40.20/G40.21 HSS in which δ_t was 0.973 and 0.977 (for two different producers) with $V_t = 0.009$ and 0.011, respectively.

Using the HSS wall thickness data collected, δ_t and V_t values were derived for ASTM A500 RHS and CHS for each source and for the aggregate data (Fig. 3-1 and Table 3-2). Figure 3-1 shows the distribution of actual-to-nominal thickness (t/t_{nom}) measurements and the average value(s) of δ_t for RHS (n = 8495) and CHS (n = 1338) compared to the CISC/CSA design wall thickness of $t = 0.90t_{nom}$. Appendix B also presents the scatter of CHS, RHS and the combined thickness coefficients of the profiles. The combined plot shows the limited range of variation between the two profiles' data sets.

Table 3-2: Summary of data for ASTM A500 HSS wall thickness

Source, i	Shape	n	δ_t	V_t
AISC (2011)	RHS	896	0.964	0.0368
Producer A	RHS	3057	0.927	0.0078
	CHS	325	0.923	0.0120
Producer B	RHS	4542	0.921	0.0118
	CHS	1013	0.930	0.0280
All	RHS	8495	0.924	0.0071
	CHS	1338	0.929	0.0170

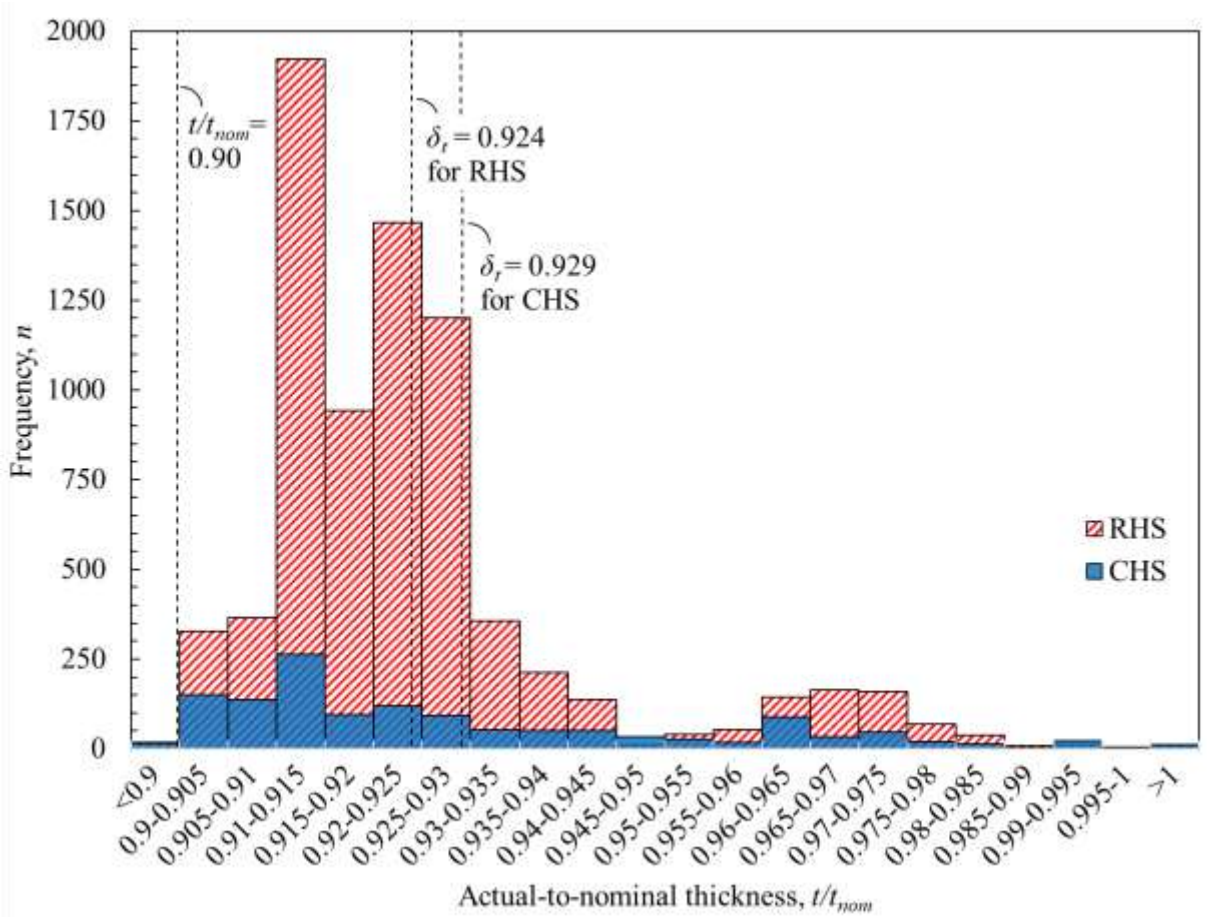

Figure 3-1: Distribution of t/t_{nom} measurements for ASTM A500 RHS and CHS.

The mean bias factors for thickness (δ_t) in Table 3-2 (and Fig. 3-1) are $\delta_t = 0.924$ and 0.929 (with $V_t = 0.007$ and 0.017) for RHS and CHS, respectively. The overall average of $\delta_t = 0.925$ with $V_t = 0.022$ (when RHS and CHS are considered together) skews close to the AISC design wall thickness of $t = 0.93t_{nom}$ (AISC, 2016; 2017), and the vast majority of t/t_{nom} ratios are above $t = 0.90t_{nom}$ (ASTM, 2023). Compared to the studies by Kennedy and Gad Aly (1980) and Schmidt and Bartlett (2002a,b) the lower average bias factor of $\delta_t = 0.925$ is expected because the focus is on ASTM A500 HSS (rather than CSA G40.20/21).

Appendix C presents and compares the actual-to-nominal thickness values for the three subsets of producer data collected for this study. Fig. C-1 presents the variation of t/t_{nom} for thickness measurements collected from an AISC study conducted by Foley and Marquez (2011) on CSA G40 HSS products. The average thickness ratio was 0.964. The higher value is to be expected when comparing to the average thickness ratios from the other two producer data sets as the G40 production standard has more rigorous tolerance parameters on thickness and mass.

Fig C-2 and Fig C-3 present the variation of the thickness ratio for the wall thickness observations obtained from Producers A and b respectively. The average thickness ratio was found to be 0.927 and 0.922 for each data set respectively. The variation in the average is a consequence of a greater ratio of CHS sections in Producer A's quality control records as compared to Producer B. From Fig 3-1, the average thickness ratio for CHS is higher than that for RHS when all the sampled thickness measurements are considered.

3.3. ADDITIONAL GEOMETRIC PROPERTIES

Bias factors for D, b, and h (δ_D, δ_b, and δ_h, respectively) for ASTM A500 HSS were derived from Producer A's QC records/measurements in Table 3-3. As shown by the statistics in Table 3-3, the actual-to-nominal outside dimension measurements for both RHS and CHS were tightly clustered around the mean values; where $\delta_D = 1.001$, $\delta_b = 1.004$ and $\delta_h = 1.000$ with corresponding COVs of $V_D = 0.007$, $V_b = 0.018$ and $V_h = 0.010$, respectively. Table 3-3 compares these values to those from Kennedy and Gad Aly (1980) for CSA G40.20/21 RHS and illustrates that, despite clear differences in δ_t for wall thickness between ASTM A500 and CSA G40.20/G40.21 HSS, the bias factors for D, b, and h are similar.

Table 3-3: Summary of additional geometric property data for ASTM A500 RHS and CHS

Source, i	Shape	n	D		b		h	
			δ_D	V_D	δ_b	V_b	δ_h	V_h
Current Study	RHS	843	-	-	1.004	0.018	1.000	0.010
	CHS	114	1.001	0.007	-	-	-	-
Kennedy and Gad Aly (1980)	RHS	149	-	-	1.002	0.003	1.002	0.003
	CHS	-	-	-	-	-	-	-

Bias factors and COVs for remaining geometric properties (i.e., the cross-sectional area, A, moment of inertia, I, radius of gyration, r, and the elastic and plastic moduli, S and Z respectively) were computed from those for t, D, b, and h above, assuming that $r_o = 2t$. Table 3-4 presents a summary of these statistics, along with the values computed by Schmidt and Bartlett (2002a) for CSA G40.20/21 HSS. Based on data obtained for the current study, it is evident that the bias factor for A (δ_A) is lower for ASTM A500 RHS than for CHS (0.93 versus 0.95). The bias factor for I (δ_I) is also slightly lower for RHS than for CHS (i.e., 0.94 vs. 0.96); however, in calculating the bias factor for r (δ_r), these effects negate one another, and $\delta_r \approx 1.0$ for both shapes.

Table 3-4: Geometric property statistics for ASTM A500 and CSA G40.20/21 HSS

Source, *i*	Shape	*n*	Cross-sectional area, *A*		Moment of inertia, *I*		Radius of gyration, *r*		Elastic Modulus, *S*		Plastic Modulus, *Z*	
			δ	*V*	*δ*	*V*	*δ*	*V*	*δ*	*V*	*δ*	*V*
Current Study	RHS	843	0.93	0.029	0.94	0.047	1.01	0.051	0.938	0.042	0.935	0.033
	CHS	114	0.95	0.115	0.96	0.104	1.00	0.011	0.943	0.060	0.939	0.061
Schmidt and Bartlett (2002)	RHS	106	0.98	0.016	0.98	0.020	1.00	0.004	0.972	0.014	0.973	0.014
	CHS	39	0.97	0.014	0.97	0.016	1.00	0.004	0.979	0.020	0.978	0.019
Kennedy and Gad Aly (1980)	RHS	200	0.98	0.034	1.00	0.032	1.01	0.020	1.002	0.031	0.981	0.033
	CHS	-	-	-	-	-	-	-	-	-	-	-

3.4. MATERIAL PROPERTIES

Liu (2016) published an extensive database of tensile test data for RHS and CHS produced to Grades B, B/C, and C between 2010 to 2012. Due to the recent harmonization of F_y in the ASTM A500 production standard, i.e., from 42 ksi and 46 ksi to 46 ksi (315 MPa) and 50 ksi (345 MPa) for ASTM A500 Grades B and C, respectively ASTM (2023), bias factors (and corresponding COVs) for Liu's study needed to be re-computed. The results, for a total of 53,097 coupons, are summarized in Table 3-5. As shown in Table 3-5, the aggregate data was evaluated according to strength grade (B, B/C and C) and profile (RHS and CHS). Statistical data for the Young's modulus, E in Table 3-5 was sourced from the same study.

Table 3-5: Summary of data for ASTM A500 HSS material properties

Grade	Shape	n	Yield Strength, F_y			Ultimate Strength, F_u			Young's Modulus, E		
			Specified Min., MPa	δ_{Fy}	V_{Fy}	Specified Min., MPa	δ_{Fu}	V_{Fu}	Average, GPa	δ_E	V_E
Grade B	RHS	31264	315	1.31	0.09	400	1.26	0.07	160	-	-
	CHS	2958	315	1.32	0.11	400	1.19	0.09	160	-	-
Grade B/C	RHS	3018	315	1.28	0.09	400	1.18	0.08	160	-	-
	CHS	568	315	1.25	0.08	400	1.14	0.06	160	-	-
Grade C	RHS	14140	345	1.24	0.09	425	1.19	0.07	160	1.04	0.05
	CHS	1149	345	1.22	0.11	425	1.17	0.08	160	1.04	0.05
Average	RHS	48422	-	1.28	0.09	-	1.21	0.07	160	1.04	0.05
	CHS	4675	-	1.26	0.10	-	1.17	0.08	160	1.04	0.05

Note: V_{Fy}, V_{Fu} and V_E = COV of F_y, F_u, and E, respectively.

The bias factors for F_y, F_u, and E (δ_{Fy}, δ_{Fu}, and δ_E, respectively) used for this study were taken as the average of the statistics for the three grades analyzed by Liu, with RHS and CHS treated separately. Table 3-6 compares these statistics to those used by Schmidt and Bartlett (2002a) and Kennedy and Gad Aly (1980) (which, again, reflect CSA G40.20/21 HSS).

Table 3-6: Summary of data for ASTM A500 HSS material properties

Source, i	Shape/ Class	n	F_y		F_u		E	
			δ_{Fy}	V_{Fy}	δ_{Fu}	V_{Fu}	δ_E	V_E
Current Study	RHS	48422	1.28	0.09	1.21	0.07	1.04	0.05
	CHS	4675	1.26	0.10	1.17	0.08	1.04	0.05
Schmidt and Bartlett (2002a)	Class C	2719	1.35	0.10	1.18	0.06	1.04	0.05
	Class H	1019	1.27	0.08	1.22	0.06	1.04	0.05
Kennedy and Gad Aly (1980)	RHS	140	1.19	0.06	-	-	-	-
	CHS	-	-	-	-	-	-	-

Chapter 4: RELIABILITY ANALYSIS

The philosophy of limit states design (load and resistance factor design) is represented by the equation (Ziemian 2010; Kulak & Grondin 2021):

$$\phi R_n \geq \sum_i^j \alpha_i S_i \tag{4-1}$$

which states that the factored resistance (or design strength), ϕR_n, must equal or exceed the effect of the factored loads, $\Sigma \alpha_i S_i$.

In the expression for design strength (ϕR_n), R_n is the nominal resistance (i.e., the strength of an element computed by using a formula in the standard, based on nominal material and geometrical properties) and ϕ is the resistance factor. The product ϕR_n reflects the uncertainties associated with the resistance, R, of a structural component. The load-effect side of the design criterion expressed by Eqn. (1) is the sum of the product(s) $\alpha_i S_i$, where S_i is the specified load effect and α_i is the corresponding load factor. The term $\Sigma \alpha_i S_i$ reflects possibility of overloading and the uncertainties inherent in the calculation of the load effect(s), S. Both resistance factors, ϕ, and load factors, α_i, are chosen to provide selected small probabilities of failure.

The probability of failure of a structural component (in bending, shear, compression, etc.) is equal to the probability that the load effect, S, is greater than the resistance R. Fig. 4-1(a) shows a set of probability density curves for S and R (dashed lines), and the prototypical normal curves (solid lines) that are used to approximate them. The region of failure, i.e., where the tails of S and R overlap, is shown therein.

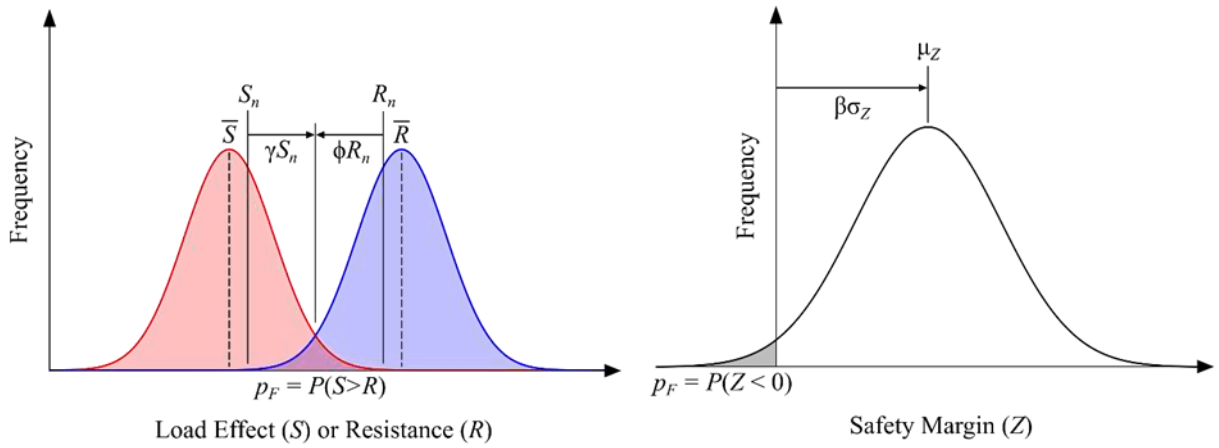

(a) load effect (S) and resistance (R) (b) safety margin (Z)

Figure 4-1: Probability density curves for (a) load effect (S) and resistance (R) and (b) safety margin (Z) [Jollymore et al. (2024)]

Load and resistance factor design (LRFD) (i.e., structural reliability theory) in North America can be traced back to the work of Cornell (1969), and the postulate that the probability of failure (p_F) may be accurately determined from the probability density curve for the safety margin (or the "performance function"), $Z = R - S$ (Fig. 4-1b) (by determining the area under the curve where $Z < 0$). This postulate, combined with the principle of constant reliability (Lind 1970), comprises the basis of first-order second-moment (FOSM) reliability methods.

FOSM reliability methods involve: (1) linear (or linearized) limit state functions (first-order); and (2) computing a notional reliability measure which is a function only of the means and variances (first and second moments) of the random variables (e.g., R and S) rather than their probability distributions (Ellingwood et al., 1980). FOSM methods (which have been used to develop LRFD criteria for steel structures) are often used because of their simplicity, and ability to treat all uncertainties in a design problem in a consistent manner.

4.1.1. Notional Probability of Failure

The LRFD criteria in Eq. (4-1) can simplistically be assumed to be comprised of two random variables, R and S, as shown in Fig. 4-1a. As described in the Introduction, a failure event occurs when $R < S$, or when $Z = R - S < 0$.

If the (arbitrary) probability density curve of the safety margin (or performance function) Z is known, then one can define a "standardized variate", U (of Z), as:

$$U = \frac{Z - \bar{Z}}{\sigma_Z} \tag{4-2}$$

where $\bar{Z}$ = mean of Z and σ_Z = standard deviation of Z. The expression that describes the probability of failure (p_F) can then be written as:

$$p_F = P\left[U < -\frac{\bar{Z}}{\sigma_Z}\right] \tag{4-3a}$$

$$= F_U\left[-\frac{\bar{Z}}{\sigma_Z}\right] \tag{4-3b}$$

where F_U = cumulative distribution function of U.

The quantity $\bar{Z}/\sigma_z$ in Eqs. (4-3a) and (4-3b), called the reliability index, β, is the number of standard deviations between and the mean value of Z ($\bar{Z}$) and the failure condition (Z = 0). This unitless measure of safety (or reliability) is called the reliability index (or, in some studies, the safety index), β (Cornell, 1969, Ang and Cornell, 1974). The greater the value of β, the greater is the reliability (where reliability = 1 – p_F) (Allen, 1991) [i.e., if σ_z remains constant, then a positive shift in $\bar{Z}$ (to the right) will reduce p_F]. This holds true for practically all probability distributions used for Z.

Eq. (4-3b) can therefore be written as:

$$p_F = F_U\left[-\beta\right] \tag{4-4}$$

According to Eq. (4-4), the safety index (β) provides a direct measure of p_F (or, conversely, reliability) if the probability distribution of Z (and hence, the real values of $\bar{Z}$ and σ_z) is known. In practice, however, the distribution(s) of R and S (and hence, Z) is invariably estimated (as shown, previously, in Fig. 4-1). When this is done, p_F [calculated from Eq. (4-4)] is referred to as the "notional" probability of failure, indicating that it should be interpreted, at best, in a comparative sense (Ellingwood et al.. 1980) (e.g., to evaluate the relative safety of various design alternatives), provided that the first- and second-moment statistics are handled consistently.

To estimate the statistics for $Z = R – S$ (i.e, $\bar{Z}$ and σ_Z) from corresponding estimates of those statistics for R and S (i.e., $\bar{R}$ and $\bar{S}$, the mean values of R and S, respectively, and σ_R and σ_S, the corresponding standard deviations), the following statistical laws must be realized (Benjamin & Cornell, 1970):

1. If R and S are random variables, $\bar{Z} = \overline{R - S} = \bar{R} – \bar{S}$.
2. Provided that R and S are independent random variables, $\sigma_Z^2 = \sigma_R^2 + \sigma_S^2$.
3. V_Z cannot be directly represented as a function of V_R and V_S.

4.1.2. NORMALLY DISTRIBUTED RANDOM VARIABLES

Based on the assumption that R and S are independent normal random variables, the probability density curve for $Z = R - S$ is also a normal curve with mean $\bar{Z} = \overline{R - S} = \bar{R} - \bar{S}$ and standard deviation (squared) $\sigma_Z^2 = \sigma_R^2 + \sigma_S^2$ (Allen, 1991; Thoft-Christensen & Baker, 1982), and the notional probability of failure p_F can be computed from the cumulative distribution function of the standard normal distribution, $\Phi[\ ]$ in accordance with Eq. (4-4):

$$p_F = \Phi\left[-\beta\right] \tag{4-5}$$

where:

$$\beta = \frac{\bar{R} - \bar{S}}{\sqrt{\sigma_R^2 + \sigma_S^2}} \tag{4-6}$$

For illustrative purposes, Table 4-1 compares notional probabilities of failure p_F computed from Eq. (4-5) to corresponding values of β.

Table 4-1: Notional probabilities of failure

Reliability Index, β	p_F
2.00	1/44
2.33	1/100
3.09	1/1000
3.54	1/5000

4.1.3. LOG-NORMALLY DISTRIBUTED RANDOM VARIABLES

According to Allen (1991), a better model for structural reliability is to replace the distributions of R and S by their natural logarithms, $\ln R$ and $\ln S$, and to fit normal curves to these distributions (such that the two tails overlap in the same way as shown in Fig 4-1a). Hence, if R and S are log-normally distributed (as implied here), then $Z = \ln R - \ln S$ is normally distributed, and:

$$\beta = \frac{\overline{\ln R} - \overline{\ln S}}{\sqrt{\sigma_{\ln R}^2 + \sigma_{\ln S}^2}} \tag{4-7a}$$

$$= \frac{\overline{\ln(R/S)}}{\sqrt{\sigma_{\ln R}^2 + \sigma_{\ln S}^2}} \tag{4-7b}$$

$$= \frac{\ln(\bar{R}/\bar{S})}{\sqrt{\sigma_{\ln R}^2 + \sigma_{\ln S}^2}} \tag{4-7c}$$

where $\overline{\ln R}$, $\overline{lnS}$, and $\overline{\ln (R/S)}$ are the mean values of ln$R$ and ln$S$ and ln(R/S), respectively, and $\sigma_{\ln R}$ and $\sigma_{\ln S}$ are the corresponding standard deviations of ln$R$ and ln$S$.

Log-normally distributed random variables can take on only positive real values, which is true-to-life for most engineering measurements [and perhaps the benefit implied by Allen (1991)].

By converting the mean values and standard deviations of ln$R$ and ln$S$ to those for R and S (i.e., through mathematical manipulation), for the log-normal case, Eq. (4-7c) for β can be written as (Thoft-Christensen & Baker 1982; Allen 1975, 1991):

$$\beta = \frac{\ln\left[\left(\bar{R}/\bar{S}\right)\sqrt{\left(1+V_S^2\right)/\left(1+V_R^2\right)}\right]}{\sqrt{\ln\left(1+V_R^2\right)\left(1+V_S^2\right)}} \tag{4-8}$$

where V_R and V_S are the coefficient(s) of variation (equal to the standard deviation divided by the mean) of R and S, respectively.

Eq. (4-8) is currently in force in CSA S6:24 (CSA 2024) to calculate β for bridges and bridge components. However, if V_R and V_S are small [i.e., according to Ellingwood et al. (1980), if V_R and V_S < about 0.30], then:

$$\beta = \frac{\ln(\bar{R}/\bar{S})}{\sqrt{V_R^2 + V_S^2}} \tag{4-9}$$

The format according to Eq. (4-9) has been long been the basis of LRFD criteria in North America (CSA 2011). However, in addition to its accuracy being dependent on the magnitudes of V_R and V_S, it is also dependent on the ratio $\bar{R}/\bar{S}$.

4.1.4. Limitations of the Small-Variance Assumption

Appendix E of the 1969 version of the CSA S16 standard (CSA 1969) (which was based on Allowable Stress) states that the basic safety factor ($\bar{R}/\bar{S}$) was taken to be 1.67, which has been successfully employed in structural steel design for several decades. That factor (1.67) has long been rounded off to 1.70 so as not to

imply an unwarranted level of precision. Table E1 of CSA (1969) indicates further variations in this factor – from 1.67 to 2.50 – based on type of stress for various elements.

4.1.5. SEPARATION FACTOR APPROACH

Eqs. (4-8) and (4-9) can be expressed in the form of a first-order second-moment (FOSM) design criteria (Cornell 1969):

$$\overline{R} \geq \theta \overline{S} \tag{4-10}$$

where θ = central safety factor [i.e., a factor that combines the uncertainties of both the resistance and load effect(s)].

In general [from Eq. (4-8)]:

$$\theta = \exp\left(\beta\sqrt{\ln\left[(1+V_R^2)(1+V_S^2)\right]}\right)\left(\sqrt{(1+V_R^2)/(1+V_S^2)}\right) \tag{4-11}$$

However, if the small-variance assumption (Ellingwood et al. 1980) holds true, then [from Eq. (4-9)]:

$$\theta = \exp\left(\beta\sqrt{V_R^2+V_S^2}\right) \tag{4-12}$$

It is advantageous to split the central safety factor, θ, into separate factors for resistance and load effect(s) – so that once a value of β is chosen (i.e., the target, β_T), ϕ for different limit states can be evaluated independently from loading uncertainties (conversely, α for different load types can be evaluated separately from other load types and independently from resistance uncertainties).

Lind (1971) showed the square-root expression in Eq. (4-12) (or any expression of two variables in that form) could be linearized by introducing a so-called separation factor (α) (not to be confused with the load factors, α_i) as follows:

$$\sqrt{V_R^2+V_S^2} \approx \alpha\left(V_R+V_S\right) \tag{4-13a}$$

where:

$$\alpha = \frac{\sqrt{1+\left(V_R / V_S\right)^2}}{1+\left(V_R / V_S\right)} \tag{4-13b}$$

For all values of $V_R/V_S \geq 0$, the separation factor, α, is restricted to the range between $\sqrt{2}/2$ and 1.0, and if V_R/V_S is near unity, α is practically constant. If V_R/V_S is restricted to the range $1/3 \leq V_R/V_S \leq 3$, α can be set equal to 0.75 with less than 6% error (Lind 1971).

Therefore, if $V_R < 0.30$ and $V_S < 0.30$ (to satisfy the small-variance assumption), and $1/3 \leq V_R/V_S \leq 3$, Eq. (10) can be written as:

$$\exp\left(-\beta\alpha V_R\right)\bar{R} \geq \exp\left(\beta\alpha V_S\right)\bar{S} \tag{4-14}$$

or as:

$$\delta_R \exp\left(-\beta\alpha V_R\right) R_n \geq \delta_S \exp\left(\beta\alpha V_S\right) S_n \tag{4-15}$$

where δ_R = bias coefficient for the resistance (= $\bar{R}/R_n$), S_n = nominal (or specified) total load effect; and δ_S = bias coefficient for the total load effect (discussed later).

Comparing the left-hand side of Eq. (4-15) to Eq. (4-1) yields the following expression for ϕ:

$$\phi = \delta_R \exp\left(-\alpha\beta V_R\right) \tag{4-16}$$

The right-hand side of Eq. (4-15) can be further separated to allow an independent treatment of the effects of different load types (as discussed later).

It is noted that Eq. (4-16) has historically been used with a separation factor of $\alpha = 0.55$ (as opposed to 0.75) to calculate ϕ [e.g., by Galambos & Ravindra (1973, 1977, 1978), Bjorhovde et al. (1978), Cooper et al. (1978), and Fisher et al. (1978), in the calibration of the original LRFD criteria]. As recently as 2010, this separation factor ($\alpha = 0.55$) was advocated by the Structural Stability Research Council (SSRC) in Appendix B.10 of the SSRC Guide (Ziemian 2010). The use of this factor can be traced to Galambos & Ravindra (1973).

4.1.6. Effect of Different Load Types

The forgoing criteria were derived by treating the load effect, S, as originating from a single load type/action acting on a structural element. However, in general, the load effect S arises due to effects from dead load (D), live load (L), wind load (W), earthquake load (E), and other actions.

In the preeminent LRFD design criteria, Galambos and Ravindra (1973) assumed the load effect *S*, for combined dead and live gravity load, to have the following form:

$$S = ET \tag{4-17a}$$

where:

$$T = \left(c_D A\right) D + \left(c_L B\right) L \tag{4-17b}$$

where D and L = random variables representing dead and live load intensities, respectively (i.e., they reflect uncertainties in idealizing loads which vary randomly in space and time by equivalent uniform distributed or concentrated design loads); c_D and c_L = deterministic influence coefficients that transform the load intensities into load effects (e.g., moment, shear, and axial force); A and B = random variable reflecting uncertainties in the transformation of the idealized design loads into load effects; and E = a random variable representing the uncertainties in structural analysis (i.e., uncertainties in modelling a three-dimensional real structure of complex geometry and behavior into a set of members and connections of fixed geometry and stipulated behavior, as well as the uncertainties induced by approximate or simplified structural analyses in lieu of complicated or refined theories). The random variable E is akin to a professional factor for loads.

Enacting the small-variance assumption, it follows that:

$$V_S = \sqrt{V_E^2 + V_T^2} \tag{4-18}$$

where V_E = COV of T and V_E = COV of E.

The COV, V_T, is related to the standard deviation, σ_T and the mean, T (i.e., $V_T = \sigma_T/\overline{T}$), and since:

$$\overline{T} = \left(c_D \overline{A}\right) \overline{D} + \left(c_L \overline{B}\right) \overline{L} \tag{4-19}$$

and:

$$V_T = \frac{\sqrt{c_D^2 \overline{A}^2 \overline{D}^2 \left(V_A^2 + V_D^2\right) + c_L^2 \overline{B}^2 \overline{L}^2 \left(V_B^2 + V_L^2\right)}}{c_D \overline{A}\,\overline{D} + c_L \overline{B}\,\overline{L}} \tag{4-20}$$

Then, by combining Eqs. (4-18) and (4-20):

$$V_S = \sqrt{V_E^2 + \frac{c_D^2 \bar{A}^2 \bar{D}^2 \left(V_A^2 + V_D^2\right) + c_L^2 \bar{B}^2 \bar{L}^2 \left(V_B^2 + V_L^2\right)}{\left(c_D \bar{A}\bar{D} + c_L \bar{B}\bar{L}\right)^2}} \tag{4-21}$$

The idea of the separation factor approach can be carried further to include the effects of multiple load types. That is, Eq. (14) can be written as:

$$\exp\left(-\beta\alpha_R V_R\right)\bar{R} \geq \exp\left(\beta\alpha_S V_S\right)\bar{S} \tag{4-22}$$

where two separation factors. αR and αS are introduced to effect a better approximation of Eq. (4-10).

Noting (as above) that:

$$V_S = \sqrt{V_E^2 + V_T^2} \tag{4-24}$$

and using a form of Eq. (4-13) again, Eq. (4-22) can be re-written as:

$$\exp\left(-\beta\alpha_R V_R\right)\bar{R} \geq \left[\exp\left(\beta\alpha_S\alpha_E V_E\right)\bar{E}\right]\left[\exp\left(\beta\alpha_S\alpha_T V_T\right)\bar{T}\right] \tag{4-23}$$

The second term in the right-hand side of Eq. (4-23) can be approximated further by using the constant and linear term(s) of the Taylor Series exponential expansion [i.e., exp(x) = 1 + x] and Eq. (4-21); i.e.:

$$\exp\left(\beta\alpha_S\alpha_T V_T\right)\bar{T} \approx \left(1 + \beta\alpha_S\alpha_T V_T\right)\left(c_D\bar{D} + c_L\bar{L}\right) \tag{4-24a}$$

$$\exp\left(\beta\alpha_S\alpha_T V_T\right)\bar{T} \approx \left(1 + \frac{\beta\alpha_S\alpha_T\sqrt{c_D^2 \bar{A}^2 \bar{D}^2 \left(V_A^2 + V_D^2\right) + c_L^2 \bar{B}^2 \bar{L}^2 \left(V_B^2 + V_L^2\right)}}{c_D\bar{A}\bar{D} + c_L\bar{B}\bar{L}}\right)\left(c_D\bar{D} + c_L\bar{L}\right) \tag{4-24b}$$

Since it is not easy to obtain information about the distributions of the random variables *A* and *B*, it was historically common to simplify the above equation(s) by taking $\bar{A} = \bar{B} = 1.0$ and CD = CL = 1.0 (which is valid for uniformly distributed dead and live loads (Jeong 1981); hence:

$$\exp\left(\beta\alpha_S\alpha_T V_T\right)\bar{T} \approx \left(1+\frac{\beta\alpha_S\alpha_T\sqrt{\bar{D}^2\left(V_A^2+V_D^2\right)+\bar{L}^2\left(V_B^2+V_L^2\right)}}{\bar{D}+\bar{L}}\right)\left(\bar{D}+\bar{L}\right) \tag{4-25}$$

By further separating the square root term in Eq. (25), the final approximation is achieved:

$$\exp\left(\beta\alpha_S\alpha_T V_T\right)\bar{T} \approx \left(1+\beta\alpha_S\alpha_T\alpha_D\sqrt{V_A^2+V_D^2}\right)\bar{D}+\left(1+\beta\alpha_S\alpha_T\alpha_L\sqrt{V_B^2+V_L^2}\right)\bar{L} \tag{4-26}$$

If Eq. (4-26) is substituted into Eq. (4-23), and the products of the α terms are denoted as $\alpha_E = \alpha_S\alpha_E$, $\alpha_D = \alpha_S\alpha_T\alpha_D$ and $\alpha_L = \alpha_S\alpha_T\alpha_L$ (in modern day, the load factors), then:

$$\exp\left(-\beta\alpha_R V_R\right)\bar{R} \geq \left[\exp\left(\beta\alpha_E V_E\right)\bar{E}\right]\left[\left(1+\beta\alpha_D\sqrt{V_A^2+V_D^2}\right)\bar{D}+\left(1+\beta\alpha_L\sqrt{V_B^2+V_L^2}\right)\bar{L}\right] \tag{4-27}$$

which implies that:

$$\phi = \delta_R\exp\left(-\alpha_R\beta V_R\right) \tag{4-28a}$$

$$\alpha_E = \exp\left(\alpha_E\beta V_E\right) \tag{4-28b}$$

$$\alpha_D = 1+\alpha_D\beta\sqrt{V_A^2+V_D^2} \tag{4-28c}$$

$$\alpha_L = 1+\alpha_L\beta\sqrt{V_B^2+V_L^2} \tag{4-28d}$$

and the approximation to the central safety factor becomes:

$$\theta_a = \frac{\exp\left(\beta\alpha_E V_E\right)\bar{E}\left[\left(1+\beta\alpha_D\sqrt{V_A^2+V_D^2}\right)\frac{\bar{D}}{\bar{L}}+\left(1+\beta\alpha_L\sqrt{V_B^2+V_L^2}\right)\right]}{\left(\frac{\bar{D}}{\bar{L}}+1\right)\exp\left(-\beta\alpha_R V_R\right)} \tag{4-29}$$

The values of α_R, α_E, α_D and α_L are chosen to minimize a function of the error in the approximation, $\varepsilon = (\theta - \theta_a)/\theta$. The function to be minimized could be the maximum error in the domain of all design situations. A design situation is characterized by the values of data variables; the ratio $c_D\bar{D}/c_L\bar{L}$, the coefficients of variation V_R, V_E, $\sqrt{V_A^2+V_D^2}$, $\sqrt{V_B^2+V_L^2}$ and β.

The ranges of data assumed in Table 4-2 were chosen. Using an error minimization process [described in Appendix B of Ravindra and Galambos (1973)], the value(s) $\alpha_R = \alpha_E = \alpha_D = \alpha_L = 0.55$ was suggested to be used, rather than an array of numerical values which changes as the number of load components change. The range of the relevant data variables in Table 4-2.

Table 4-2: Ranges of data variables (Galambos and Ravindra, 1973)

Variable	Range
V_R	0.10 – 0.15
V_E	0.05 – 0.15
$\sqrt{V_A^2 + V_D^2}$	0.02 – 0.10
$\sqrt{V_B^2 + V_L^2}$	0.10 – 0.40
$c_D\bar{D}/c_L\bar{L}$	1.0 – 4.0
β	3.0 – 4.0

This format was used extensively in the calibration of steel design codes in the 1970s and 1980s.

4.2. FORM APPROACH

Resistance factors may be determined to achieve target reliability indices using the first order reliability method (FORM), which remains the basis of the more accurate reliability formulations available. Representative factored load effects are calculated for the load effect fractions obtained from Step 3 of the general procedure described in Clause B.2.2 of CSA S408-11 (2011) using the load factors and load combinations from the relevant standard. Resistance factor values are assumed, the associated nominal resistances are calculated and, using the statistical data obtained from Steps 1 and 2 in Clause B.2.2 of CSA S408-11 (2011), the corresponding reliability indices are calculated. An example of this procedure is presented in Kariyawasam et al. (1997). An advanced first order reliability method based on non-linear performance functions is used in Clause C.11 to determine the reliability index.

4.2.1. APPROXIMATE FORM APPROACH

As an alternative to FORM, the resistance factor to be used with load factors and load combinations can be derived as (Kennedy & Baker 1984; Nowak & Lind 1979):

$$\phi = \delta_R \frac{\sum_i \alpha_i S_i}{S_m} \exp\left(-\beta_T \sqrt{V_R^2 + V_S^2}\right) \tag{4-30}$$

The above assumes log-normally distributed variables with small-variance. Removing the latter assumption, it can be written as (Barker et al. 1991):

$$\phi = \delta_R \frac{\sum \alpha_i S_i}{S} \exp(-\beta \sqrt{V_R{}^2 + V_S{}^2}) \tag{4-31}$$

Considering live and dead load only, and making β the subject;

$$\beta = \frac{1}{\sqrt{V_R{}^2 + V_S{}^2}} \ln\left[\frac{\delta_R}{\phi} \frac{\alpha_D + \alpha_L \left(L/D\right)}{\delta_D + \delta_L \left(L/D\right)}\right] \tag{4-32}$$

The first AASHTO specifications were based on the FOSM principles. Assuming log-normal distribution for the resistance and load effect(s) and applying a similar procedure to that above (Barker et al., 1991):

$$\phi = \delta_R \frac{\sum \alpha_i S_i}{\theta \bar{S}} \tag{4-33}$$

$$\theta = \exp\left(\beta \sqrt{\ln\left[(1+V_R^2)(1+V_S^2)\right]}\right)\left(\sqrt{(1+V_R^2)/(1+V_S^2)}\right) \tag{4-34}$$

Chapter 5: RESISTANCE AND LOADING STATISTICS

5.1. RESISTANCE

If the nominal load effects (S_i) and the associated load factors (α_i) are specified, an appropriate resistance factor (ϕ) can be calculated for a target reliability index (β) (or, inversely, given ϕ, β can be determined) according to eqn. (4-31), where S and V_S = mean and COV of the total load effect, respectively, and δ_R and V_R = bias factor and COV of the resistance R, derived from the following model:

$$R = (GMP)d \tag{5-1}$$

For R, we can utilize the resistance function approaches developed in EN 1990 Annex D to produce the equations for bias coefficients and coefficients of variation. The quantity in parentheses in Eq. (5-1) represents the resistance model originally proposed by Galambos and Ravindra (1981). Considering the simple product function for R, where P represents a professional factor, M a material factor, G a geometric factor and d a discretization factor.

The professional factor represents the scale of the model error. The bias coefficient for the professional factor is calculated from the actual-to-nominal (predicted) strength, or the average test-to-predicted ratio. Professional factor statistical parameters used in this study were obtained from the research conducted by Bjorhovde and Birkemoe (1979) using full scale column and stub column tests. Appendix A graphically presents the results of that study. The statistical parameters for the professional factor utilized in this study are drawn from the results for Class C HSS presented in Fig A-1, with a column curve parameter n = 1.34.

If these factors are taken to be independent variables, the resistance bias coefficient is simply given by the product of the bias coefficients of the independent variables, i.e:

$$\delta_R = \delta_G \delta_M \delta_P \delta_d \tag{5-2}$$

and for the coefficient of variation:

$$V_R^2 = \left[\prod_{i=1}^{j} \left(V_{X_i}^2 + 1 \right) \right] - 1 \tag{5-3}$$

Using the small variance assumption simplifies the formula for the coefficient of variation to a square root of sum of squares form, i.e.:

$$V_R = \sqrt{\sum_{i=1}^{j} (V_{X_i}{}^2)} \tag{5-4}$$

which further simplifies to a square root of sum of squares form, i.e.:

$$V_R = \sqrt{V_G^2 + V_M^2 + V_P^2 + V_d^2} \tag{5-5}$$

where δ_G, δ_M, δ_P, and δ_d are the bias factors for G, M, P and d, respectively, and V_G, V_M, V_P, and V_d are the associated COVs.

The statistical parameters for d were taken as $\delta_d = 1.04$ and $V_d = 0.033$ for HSS members (Schmidt and Bartlett, 2002b), and professional factor statistics, which depend on λ, were collected from the same study. λ is a non-dimensional slenderness parameter given as:

$$\lambda = \frac{KL}{r}\sqrt{\frac{F_y}{\pi^2 E}} \tag{5-6}$$

where K = effective length factor, and L = unbraced column length.

Because professional factors are computed using actual/measured (rather than nominal) material and geometric properties, the statistics are valid for both ASTM A500 and CSA G40.20/21 HSS.

5.1.1. Axial Compression

The factored axial compressive resistance formula specified in Clause 13.3.1.1 of CSA S16:24 (2024) is given as:

$$C_r = \frac{\phi A F_y}{\left(1+\lambda^{2n}\right)^{\frac{1}{n}}} \tag{5-7}$$

where, the resistance factor $\phi = 0.90$, and:

$$\lambda = \sqrt{\frac{F_y}{F_e}} \tag{5-8}$$

For compression members designed according to CSA S16:24 (2024) Clause 13.3, resistance statistics can be computed from Eqs. (4-33) and (4-34), with M as:

$$M = F_y \left[1 + \lambda^{2n}\right]^{-1/n} \tag{5-9}$$

where n = column curve parameter (= 1.34 for ASTM A500 and CSA G40.20/21 Class C HSS) and λ = non-dimensional slenderness parameter, given in Eq. 5-6.

Assuming that KL and n are deterministic, it can be shown that, as per Schmidt and Bartlett (2002b):

$$\delta_M = \delta_{F_y} \frac{\left[1 + (\lambda\delta_\lambda)^{2n}\right]^{-1/n}}{\left[1 + \lambda^{2n}\right]^{-1/n}} \tag{5-10}$$

where:

$$\delta_\lambda = \frac{1}{\delta_r}\sqrt{\frac{\delta_{F_y}}{\delta_E}} \tag{5-11}$$

As shown by Schmidt (2000):

$$V_M = \sqrt{\frac{T_1^2 V_{F_y}^2 + T_2^2 V_r^2 + T_3^2 V_E^2}{W^2}} \tag{5-12}$$

where:

$$W = \left[1 + (\lambda\delta_\lambda)^{2n}\right]^{-1/n} \tag{5-13}$$

The coefficients T_1, T_2, and T_3 in Eqs. (5-14), (5-15) and (5-16) – termed "participation factors" – are functions of the partial derivatives of Eq. (5-10) with respect to F_y, r, and E, respectively, evaluated at the mean values F_y, E, and r:

$$T_1 = \left[1 + (\lambda\delta_\lambda)^{2n}\right]^{-(n+1)/n} \quad (5\text{-}14)$$

$$T_2 = 2(\lambda\delta_\lambda)^{2n}\left[1 + (\lambda\delta_\lambda)^{2n}\right]^{-(n+1)/n} \quad (5\text{-}15)$$

$$T_3 = (\lambda\delta_\lambda)^{2n}\left[1 + (\lambda\delta_\lambda)^{2n}\right]^{-(n+1)/n} \quad (5\text{-}16)$$

The variation of δ_M and V_M with respect to λ is shown in Figs. 5-1(a) and (b), respectively, for ASTM A500 RHS and CHS assuming that $t = 1.00t_{nom}$. Therein, it is observed that for low slenderness parameters, i.e., $\lambda < 0.4$, column strength is dominated by yielding of the cross-section, and therefore $\delta_M \approx \delta_{Fy}$ and $V_M \approx V_{Fy}$. As λ increases, the failure mode changes to inelastic buckling and subsequently to elastic buckling until, for $\lambda > 2$, $\delta_M \approx \delta_E\delta_r^2$ and $V_M \approx \sqrt{(V_E^2 + 4V_r^2)}$. Similar curves for CSA G40.20/21 Class C and Class H HSS using data from Schmidt and (2002b) are also provided, for comparison.

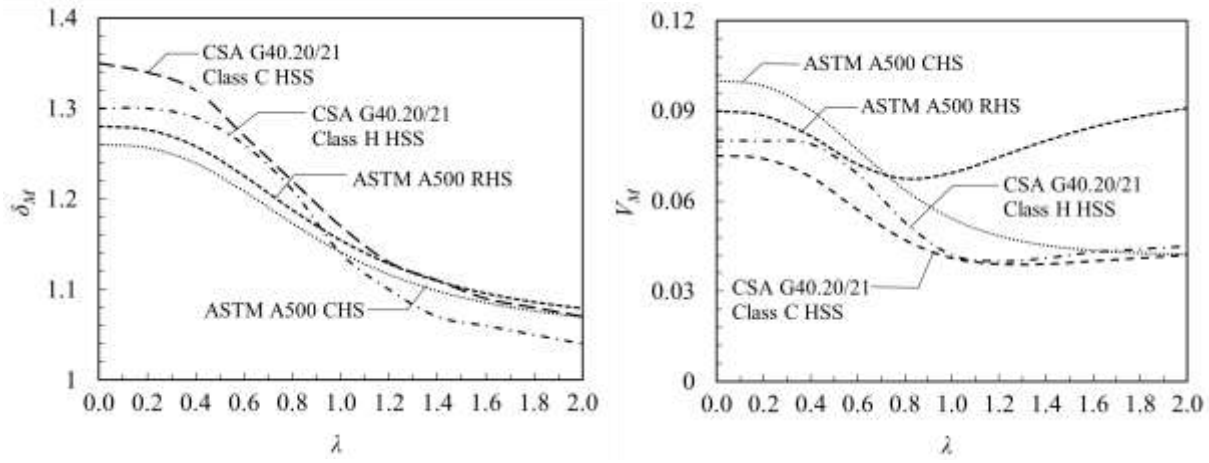

(a) (b)

Figure 5-1: Variation in (a) δ_M and (b) V_M with respect to λ for ASTM A500 and CSA G40.20/21 HSS for $t = 1.00t_{nom}$

5.1.2. AXIAL TENSION

The factored axial tension resistance formula specified in Clause 13.3.1.1 of CSA S16:24 (2024) is given as:

$$T_r = \phi A_g F_y \quad (5\text{-}17a)$$

where the resistance factor ϕ = 0.90. Similarly, the resistance function can be modelled as a product function as proposed by Galambos and Ravindra (1981), and the resistance statistics determined from Eqs. (5-2) and (5-5), above.

Additionally, tensile failure through net section fracture was considered as part of this study. The factored tensile resistance in net section fracture is given as:

$$T_r = \phi_u A_n F_u \tag{5-17b}$$

where the resistance factor, ϕ_u = 0.75.

5.1.3. LATERALLY SUPPORTED BENDING

Statistical parameters for laterally supported bending members are determined for Class 1, 2 and 3 members, for a resistance factor ϕ = 0.90. For Class 1 and 2, the factored moment resistance is given by:

$$M_r = \phi Z F_y \tag{5-18}$$

So, for Class 1 and 2 laterally supported bending members, the bias coefficient of the resistance is given by:

$$\delta_R = \delta_Z \delta_{F_y} \delta_P \delta_d \tag{5-19}$$

and the COV is:

$$V_R = \sqrt{V_Z^2 + V_{F_y}^2 + V_P{}^2 + V_d{}^2} \tag{5-20}$$

The maximum capacity of laterally supported Class 3 beams is limited to the yield moment, such that:

$$M_r = \phi S F_y \tag{5-21}$$

So, for Class 3 laterally supported bending members, the bias coefficient of the resistance is given by:

$$\delta_R = \delta_S \delta_{F_y} \delta_P \delta_d \tag{5-22}$$

and the COV is:

$$V_R = \sqrt{V_S^2 + V_{F_y}^2 + V_P{}^2 + V_d{}^2} \tag{5-23}$$

5.2. LOADING STATISTICS

It is useful to normalize the reliability index (β) [Eq. (4-32)] over the live-to-dead load ratio (L/D). Considering the basic load combination of $D + L$ due to use and occupancy, with load factors (α_i) from the National Building Code of Canada (NBCC, 2020) of 1.25 and 1.5, respectively, Eq. (4-32) becomes:

$$\beta = \frac{1}{\sqrt{V_R^2 + V_S^2}} \ln\left[\frac{\delta_R}{\phi}\left(\frac{1.25 + 1.5(L/D)}{\delta_D + \delta_L(L/D)}\right)\right] \tag{5-24}$$

where δ_D and δ_L = bias factors for dead and live load, respectively.

According to Annex B of CSA S16:24, the compression member design provisions in Clause 13.3.1.1 of CSA S16 target $\beta = 3.0$ (for ductile failures) with a resistance factor $\phi = 0.90$. Similarly, the target $\beta = 3.0$ is applicable to tension failure (gross section yielding) and laterally supported bending, while $\beta = 4.0$ applies to net section fracture in tension (brittle failure).

In this study, D was assigned $\delta_D = 1.05$ and $V_D = 0.10$ in accordance with Ellingwood et al. (1980) and, as described in Appendix 1 of Schmidt and Bartlett (2002b), and δ_L and V_L were assigned values of 0.78 and 0.32, respectively, for a 30-year reference period.

In the section that follows, β values are calculated for ASTM A500 HSS compression members over the range $0 \leq \lambda \leq 2$ using $t = 0.90$, 0.93, and $1.00t_{nom}$ and the resulting β values are compared to both (i) the target value of β, and (ii) the inherent reliability index attained for CSA G40.20.21 Class C and H members computed using the data from Schmidt and Bartlett (2002b) (with $t = 1.00t_{nom}$).

Similarly, the reliability of members in tension and laterally supported bending was also assessed over the same practical range, and the results are presented in comparison with G40 member results obtained by Schmidt and Bartlett (2002).

5.3. PROFESSIONAL AND DISCRETIZATION STATISTICS

5.3.1. COMPRESSION MEMBERS

5.3.1.1. PROFESSIONAL STATISTICS

Professional factor statistics for members in compression were collected from the study by Schmidt and Bartlett (2002) on CSA G40.20/21 HSS members. The results used in that study were drawn from the full-scale testing program conducted by Bjorhovde and Birkemoe (1979), which was conducted to the stated range for the slenderness parameter. Because professional factors are computed using actual/measured (rather than nominal) material and geometric properties, the statistics are valid for both ASTM A500 and CSA G40.20/21 HSS. The value of the bias factor and COV for the professional factor both depend on λ. As the statistics obtained range between $0 \leq \lambda \leq 2$, the resistance statistics computed also correspond to this range. Appendix A presents graphs produced by Schmidt and Bartlett (2002) from the results of Bjorhovde and Birkemoe (1979). The graphs present the variation of the professional factor statistics for Class C and Class H HSS.

The bias factor of the material factor, denoted by δ_M is constant for $\lambda > 2$ and is given roughly by $\delta_E\delta_r^2$. The coefficient of variation of the material factor, V_M is also constant over this range of λ, given roughly by $(V_E^2 + 4V_R^2)^{1/2}$ (Schmidt and Bartlett, 2002). The work of Kennedy and Gad Aly (1980) on limit states design of steel structures also shows that the material factor statistics tend towards a constant value for a slenderness parameter greater than 2.

The typical range of λ for HSS columns is up to 1.5 (Ziemian, 2010). This limit is a consequence of the CSA classification of columns based on slenderness. As per Clause 10.4.2.1 of the CSA S16:24 handbook, the slenderness ratio of a compression member shall not exceed 200, i.e. $KL/r < 200$. This value corresponds to $\lambda < 2.6$. Even so, for HSS building columns the common slenderness range is $35 \leq KL/r \leq 95$, corresponding to a slenderness parameter range of $0.5 \leq \lambda \leq 1.25$. As such, the range of λ considered in this study is satisfactory. The professional factor statistical parameters used in this study are show in Table 5-1 below.

Table 5-1: Professional factors for compression members [Schmidt and Bartlett (2002b), Bjorhovde and Birkemoe (1979)]

Slenderness Parameter, λ	Professional bias factor, δ_P	Coefficient of variation, V_P
0.0	1.00	0.000
0.2	1.01	0.028
0.4	1.01	0.028
0.6	1.03	0.096
0.8	1.09	0.066
1.0	1.14	0.011
1.2	1.13	0.095
1.4	1.08	0.089
1.6	1.04	0.039
1.8	1.03	0.035
2.0	1.02	0.030

5.3.1.2. DISCRETIZATION STATISTICS

Discretization accounts for the tendency in design to round up to the next suitable section size that is commercially available. A discrete number of steel shapes produced must resist a continuum of demands due to loads. As a result, elements are often slightly conservative compared to the intended resistance capacity. The discretization parameters account for this over-estimation of the resistance.

Schmidt and Bartlett (2002b) promulgate a system for developing the discretization statistics of steel sections. By comparing assumed demands against member resistance capacities specified in the CISC Handbook of Steel Construction (2000) selection tables, and selecting only the most efficient sections for each assumed demand, i.e. sections meeting the demand with the least weight, they obtained the ratio of demand to capacity. Working from this actual-to-nominal ratio, discretization parameters were obtained, similar to how this study develops the statistics for the thickness measurements.

The statistical parameters for d in compression were taken as $\delta_d = 1.04$ and $V_d = 0.033$ for HSS compression members, drawn from Schmidt and Bartlett (2002b).

5.3.2. TENSION MEMBERS

5.3.2.1. PROFESSIONAL STATISTICS

Professional statistics for tension failure through yielding of the gross cross section were obtained as $\delta_P = 1.0$ and $V_P = 0$, from the research of Bjorhovde and Birkemoe (1979). Class C and H members were analysed using specially designed fixtures intended to simulate pin-ended conditions. The capacities of the long columns analysed were normalised using stub column capacities and the results reported for a range of λ values. Clusters of results for λ in the range of $0.4 \leq \lambda \leq 1.5$ were obtained. Professional factor statistics were obtained by

analysing the results of clusters of λ values, while the parameters for those values of λ not represented were approximated. For tension failure through net section fracture, the same were obtained as 1.006 and 0.049, respectively.

5.3.2.2. DISCRETIZATION STATISTICS

Discretization statistics in tension (both yielding and fracture) were drawn from Schmidt and Bartlett (2002b) and these were the same as the statistics for the axial compression analysis, with $\delta_d = 1.04$ and $V_d = 0.033$.

5.3.3. BENDING MEMBERS

5.3.3.1. PROFESSIONAL STATISTICS

Professional statistics for laterally supported bending members are drawn from the work of Bjorhovde and Birkemoe (1979) and cited by Kennedy and Gad Aly (1980). The derivation of the professional statistics is as discussed in 5.3.1.1 above. The same statistics were used in the study by Schmidt and Bartlett (2002b). Class 1 and 2 members were noted to have $\delta_P = 1.1$ and $V_P = 0.11$, while Class 3 members have $\delta_P = 1.07$ and $V_P = 0.06$.

5.3.3.2. DISCRETIZATION STATISTICS

Discretization statistics in bending were again drawn from the research of Schmidt and Bartlett (2002b), with $\delta_d = 1.04$ and $V_d = 0.028$.

5.4. RESISTANCE STATISTICS

5.4.1. COMPRESSION MEMBERS

From Eqs. (5-2) and (5-5), using the above-stated statistics, the resistance statistics in compressions were computed. The results are presented in Table 5-2 below over the slenderness parameter range of $0 \leq \lambda \leq 2$.

Table 5-2: Summary of final resistance statistical parameters for ASTM A500 HSS in compression

λ	Shape	$t = 0.90t_{nom}$		$t = 0.93t_{nom}$		$t = 1.00t_{nom}$	
		δ_R	V_R	δ_R	V_R	δ_R	V_R
0	RHS	1.37	0.101	1.33	0.101	1.24	0.100
	CHS	1.38	0.170	1.34	0.165	1.25	0.156
0.2	RHS	1.38	0.104	1.34	0.103	1.25	0.103
	CHS	1.39	0.171	1.35	0.166	1.26	0.158
0.4	RHS	1.36	0.100	1.32	0.099	1.23	0.098
	CHS	1.37	0.166	1.33	0.162	1.24	0.153
0.6	RHS	1.34	0.138	1.30	0.136	1.22	0.134
	CHS	1.36	0.184	1.32	0.180	1.23	0.172
0.8	RHS	1.37	0.124	1.34	0.121	1.25	0.116
	CHS	1.40	0.165	1.36	0.161	1.27	0.151
1.0	RHS	1.39	0.109	1.36	0.105	1.28	0.097
	CHS	1.42	0.149	1.38	0.144	1.29	0.133
1.2	RHS	1.35	0.161	1.31	0.157	1.24	0.148
	CHS	1.38	0.176	1.34	0.171	1.25	0.162
1.4	RHS	1.27	0.163	1.23	0.158	1.16	0.149
	CHS	1.29	0.173	1.26	0.168	1.18	0.158
1.6	RHS	1.20	0.137	1.17	0.131	1.10	0.120
	CHS	1.23	0.154	1.20	0.148	1.12	0.137
1.8	RHS	1.18	0.139	1.15	0.133	1.08	0.122
	CHS	1.21	0.153	1.17	0.148	1.10	0.136
2.0	RHS	1.16	0.140	1.13	0.134	1.07	0.122
	CHS	1.19	0.153	1.15	0.147	1.08	0.135

5.4.2. TENSION MEMBERS

From equations (5-2) and (5-5), using the above-stated statistics, the resistance statistics in tension were computed. The results are presented in Table 5-3 below.

Table 5-3: Summary of final resistance statistical parameters for ASTM A500 HSS in tension

Condition	Shape	$t = 0.90t_{nom}$		$t = 0.93t_{nom}$		$t = 1.00t_{nom}$	
		δ_R	V_R	δ_R	V_R	δ_R	V_R
Gross section yielding	RHS	1.33	0.100	1.37	0.100	1.24	0.100
	CHS	1.38	0.124	1.34	0.124	1.25	0.123
Net section fracture	RHS	1.30	0.096	1.26	0.096	1.18	0.096
	CHS	1.29	0.119	1.25	0.119	1.17	0.118

5.4.3. LATERALLY SUPPORTED BENDING MEMBERS

From equations (5-2) and (5-5), using the above-stated statistics, the resistance statistics for members in laterally supported bending were computed. The results are presented in Table 5-4 below.

Table 5-4: Summary of final resistance statistical parameters for ASTM A500 HSS in bending

Section Classification	Shape	$t = 0.90t_{nom}$		$t = 0.93t_{nom}$		$t = 1.00t_{nom}$	
		δ_R	V_R	δ_R	V_R	δ_R	V_R
Class 1, 2	RHS	1.50	0.149	1.46	0.149	1.37	0.149
	CHS	1.52	0.163	1.47	0.163	1.38	0.163
Class 3	RHS	1.46	0.119	1.42	0.119	1.34	0.119
	CHS	1.50	0.126	1.45	0.126	1.36	0.126

Chapter 6: RESULTS

In the section that follows, β values are calculated for ASTM A500 HSS compression members with $0 \leq \lambda \leq 3$ using $t = 0.90$, 0.93, and $1.00t_{nom}$ and the resulting β values are compared to both (i) the target reliability index, and (ii) the inherent reliability index attained for CSA G40.20.21 Class C and H members computed using the data from [8] (with $t = t_{nom}$). Results are then discussed over the practical range of $1 \leq L/D \leq 3$.

6.1. COMPRESSION MEMBERS

Figures 6-1 to 6-6 depict the calculated β values as a function of L/D where Figs. 6-1, 6-2 and 6-3 present the results for ASTM A500 RHS analyzed at $t = 0.90$, 0.93 and $1.00t_{nom}$ respectively, and Figs. 6-4, 6-5 and 6-6 present the same for CHS. Therein, the solid black lines represent the average β for all sections analysed, the grey shaded regions represent the average β for each λ value considered, and the target $\beta = 3.0$ is indicated by a dashed horizontal line.

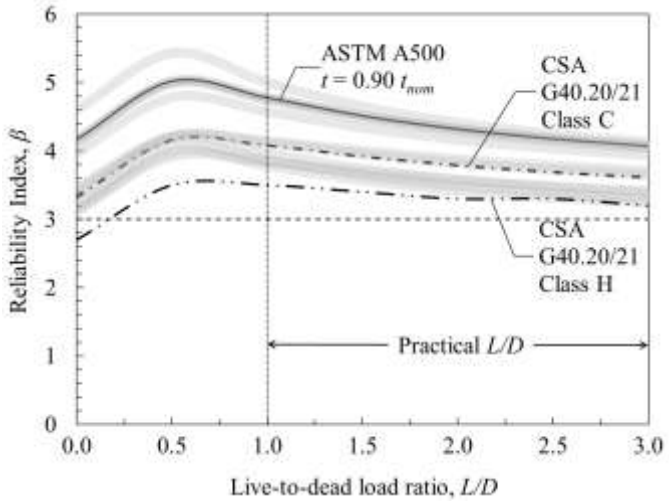

Figure 6-1: β vs. L/D ratio for CSA G40.20/21 HSS Class C and H vs. ASTM A500 RHS with $t = 0.90t_{nom}$

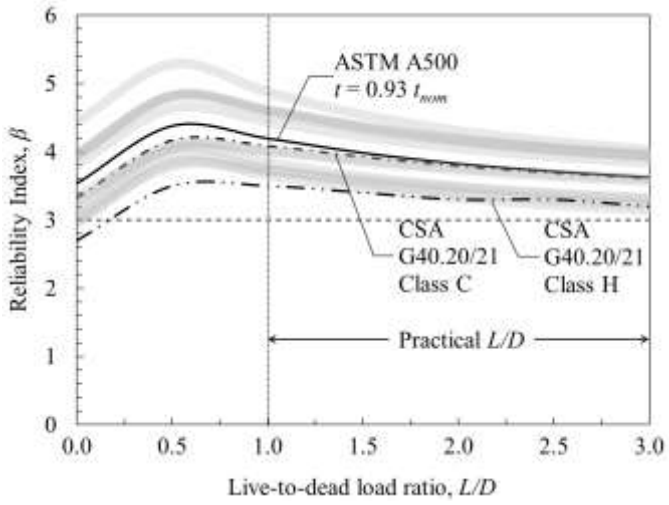

Figure 6-2: β vs. L/D ratio for CSA G40.20/21 HSS Class C and H vs. ASTM A500 RHS with $t = 0.93t_{nom}$

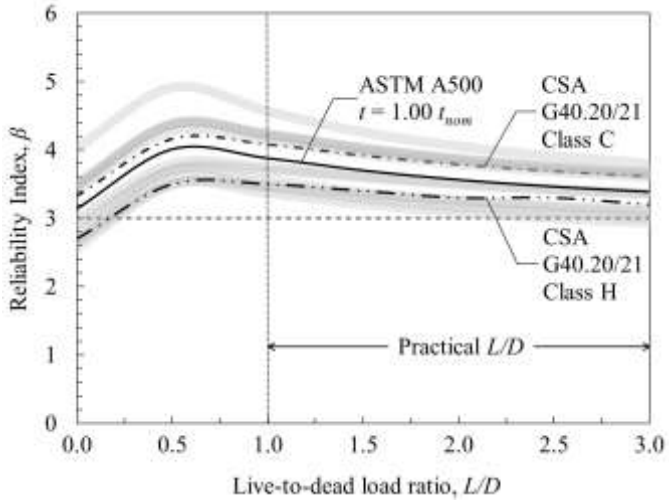

Figure 6-3: β vs. L/D ratio for CSA G40.20/21 HSS Class C and H vs. ASTM A500 RHS with $t = 1.00t_{nom}$

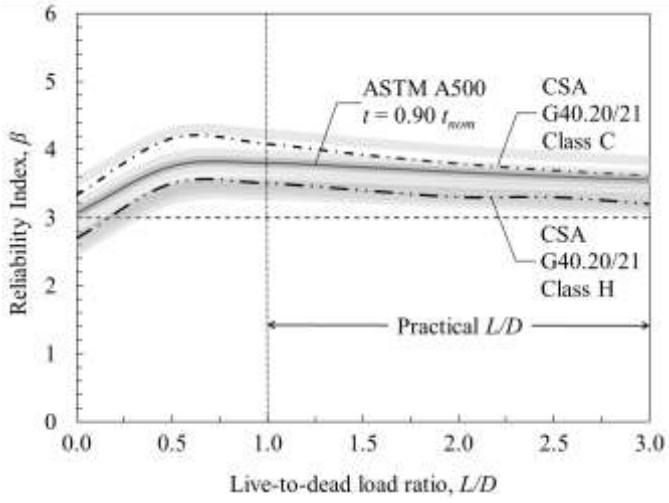

Figure 6-4: β vs. L/D ratio for CSA G40.20/21 HSS Class C and H vs. ASTM A500 CHS with $t = 0.90t_{nom}$

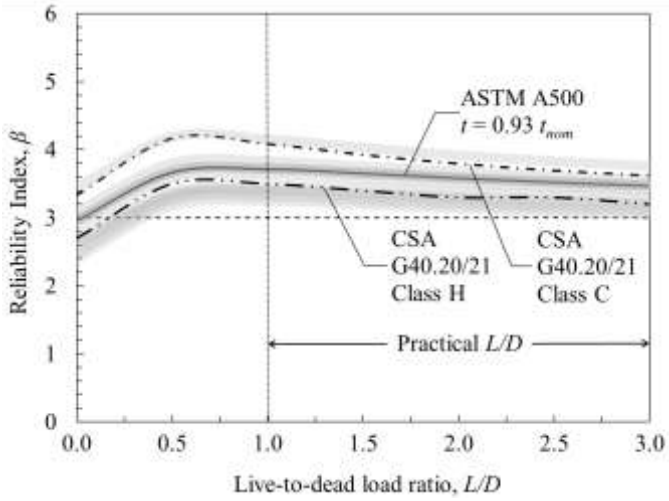

Figure 6-5: β vs. *L/D* ratio for CSA G40.20/21 HSS Class C and H vs. ASTM A500 CHS with $t = 0.93t_{nom}$

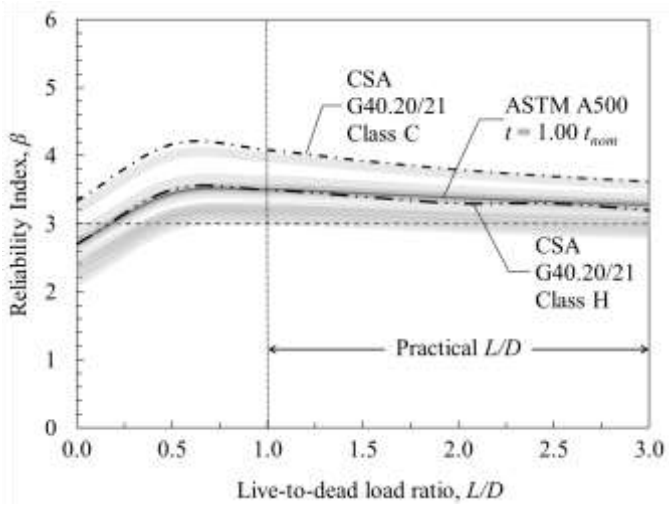

Figure 6-6: β vs. *L/D* ratio for CSA G40.20/21 HSS Class C and H vs. ASTM A500 CHS with $t = 1.00t_{nom}$

FORM analysis over the practical range of live-to-dead *(L/D)* load ratios ($1 \leq L/D \leq 3$) against the axial compressive resistance specified by Clause 13.1.1.1 of CSA S16:24 shows that $t = 0.90$, 0.93, and $1.00t_{nom}$ all provide reliability indices (β) above the target (i.e., $\beta > 3.0$) for RHS and CHS compression members made to ASTM A500.

The current ASTM A500 design wall thickness given by CSA and the CISC ($t = 0.90t_{nom}$) is conservative for HSS members in compression. It would be justified to adopt a design wall thickness of $t = 0.93t_{nom}$ in compression to harmonize CSA S16's requirements with AISC 360, for consistency across standards.

For maximum economy, a design wall thickness of $t = 1.00t_{nom}$ for A500 HSS compression members may also be justified.

6.2. TENSION MEMBERS

Figures 6-7, 6-8 and 6-9 depict the calculated β values as a function of *L/D* for RHS under gross section yielding. Figures 6-10, 6-11 and 6-12 present the same for RHS under net section fracture. Therein, the solid black lines represent the average β for all sections analysed, and the target β is indicated by a dashed horizontal line. The results of the analysis are presented side-by-side with the results of the G40.20/21 study conducted by Schmidt and Bartlett (2002b).

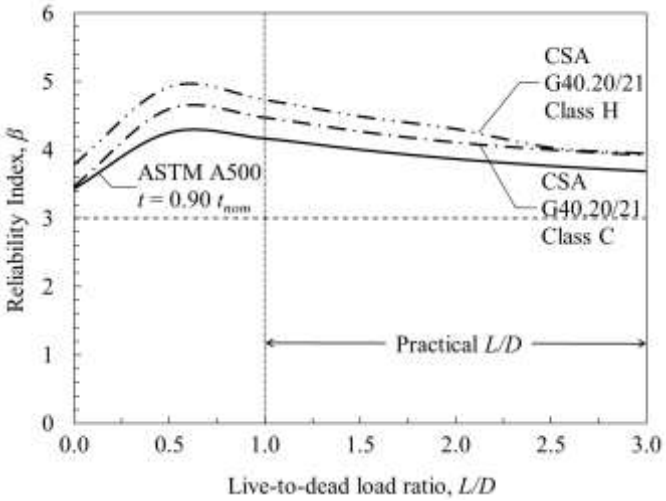

Figure 6-7: β vs. *L/D* ratio for CSA G40.20/21 HSS Class C and H vs. ASTM A500 RHS with $t = 0.90t_{nom}$ examined for gross section yielding

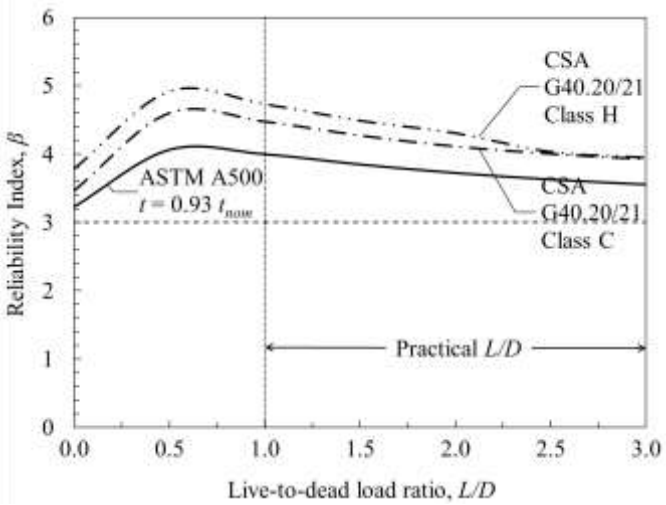

Figure 6-8: β vs. *L/D* ratio for CSA G40.20/21 HSS Class C and H vs. ASTM A500 RHS with $t = 0.93t_{nom}$ examined for gross section yielding

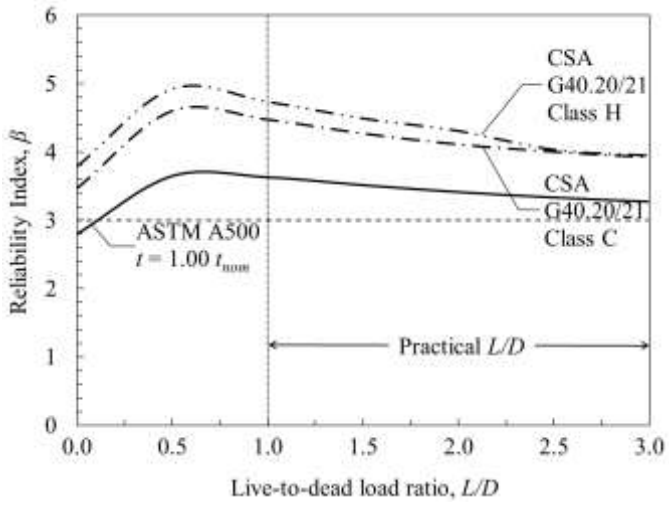

Figure 6-9: β vs. L/D ratio for CSA G40.20/21 HSS Class C and H vs. ASTM A500 RHS with $t = 1.00t_{nom}$ examined for gross section yielding

The reliability index analysis for axial tensile resistance for gross yielding failure of RHS members shows that $t = 0.90$, 0.93, and $1.00t_{nom}$ all provide reliability indices (β) above the target.

The current ASTM A500 design wall thickness given by CSA and the CISC ($t = 0.90t_{nom}$) is conservative for RHS members in axial tension when the failure criteria of gross section yielding is considered. It would be justified to adopt a design wall thickness of $t = 0.93t_{nom}$ for gross section yielding to harmonize CSA S16's requirements with AISC 360, for consistency across standards. For maximum economy, a design wall thickness of $t = 1.00t_{nom}$ for A500 RHS members under gross section yielding tension may also be justified.

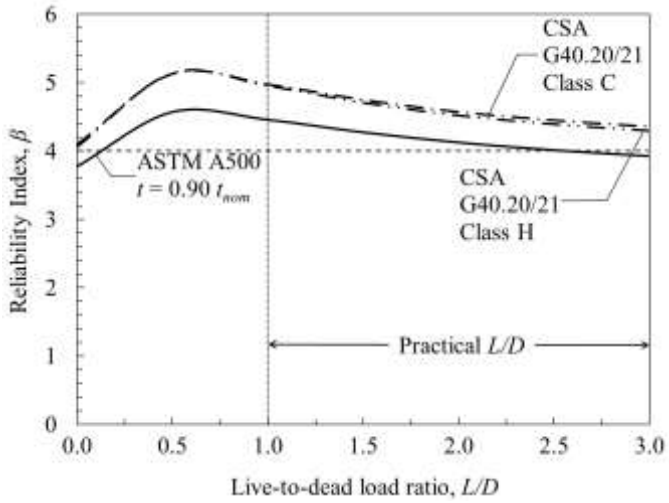

Figure 6-10: β vs. L/D ratio for CSA G40.20/21 HSS Class C and H vs. ASTM A500 RHS with $t = 0.90t_{nom}$ examined for net section fracture

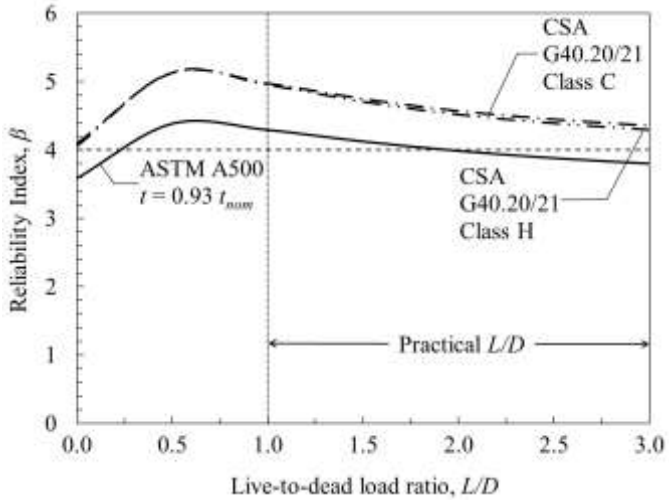

Figure 6-11: β vs. L/D ratio for CSA G40.20/21 HSS Class C and H vs. ASTM A500 RHS with $t = 0.93t_{nom}$ examined for net section fracture

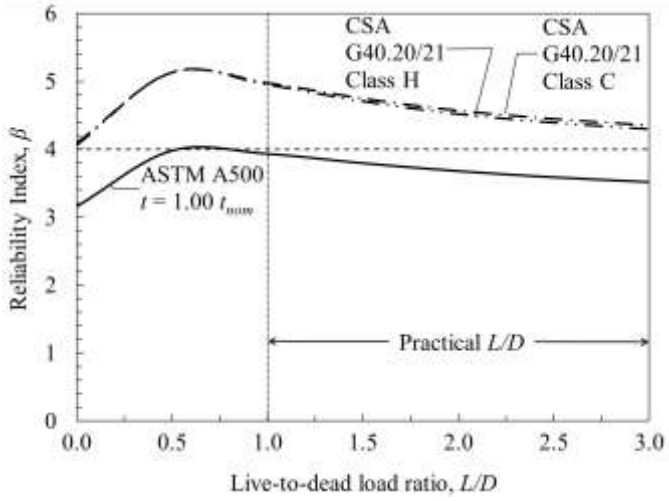

Figure 6-12: β vs. L/D ratio for CSA G40.20/21 HSS Class C and H vs. ASTM A500 RHS with $t = 1.00t_{nom}$ examined for net section fracture

RHS under net section fracture displays a reliability index that dips below the target reliability index of 4.0 at high values of L/D (> 2.5) when considering the design thickness of $0.90t_{nom}$, and L/D > 2.0 for the design thickness of $0.93t_{nom}$. Such high live-to-dead load ratios are uncommon in practical design considerations and as such these design thickness values can be taken as meeting the target for typical design load ratio considerations.

Figures 6-13, 6-14 and 6-15 depict the calculated β values as a function of L/D for CHS under gross section yielding. Figures 6-16, 6-17 and 6-18 present the same for CHS under net section fracture. Therein, the solid black lines represent the average β for all sections analysed, and the target β = 3.0 is indicated by a dashed horizontal line. The results of the analysis are presented side-by-side with the results of the G40.20/21 study conducted by Schmidt and Bartlett (2002).

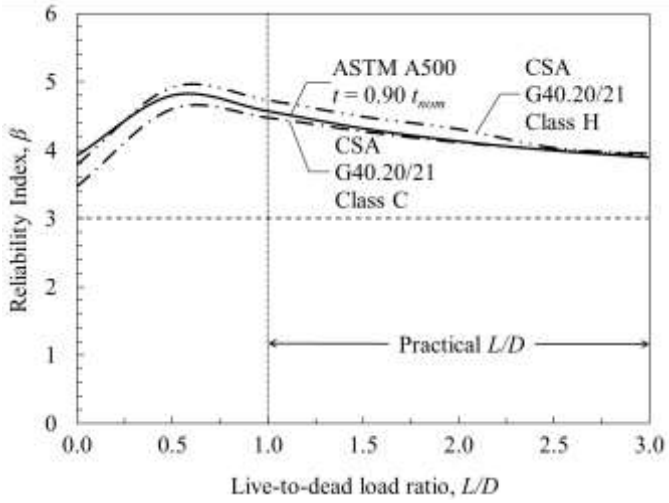

Figure 6-13: β vs. L/D ratio for CSA G40.20/21 HSS Class C and H vs. ASTM A500 CHS with $t = 0.90t_{nom}$ examined for gross section yielding

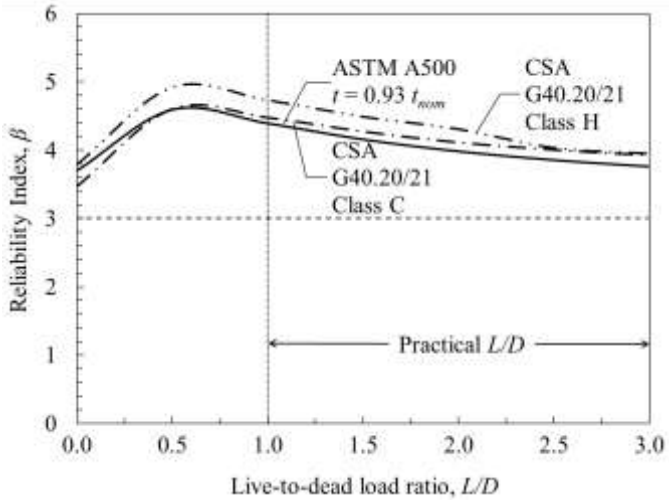

Figure 6-14: β vs. L/D ratio for CSA G40.20/21 HSS Class C and H vs. ASTM A500 CHS with $t = 0.93t_{nom}$ examined for gross section yielding

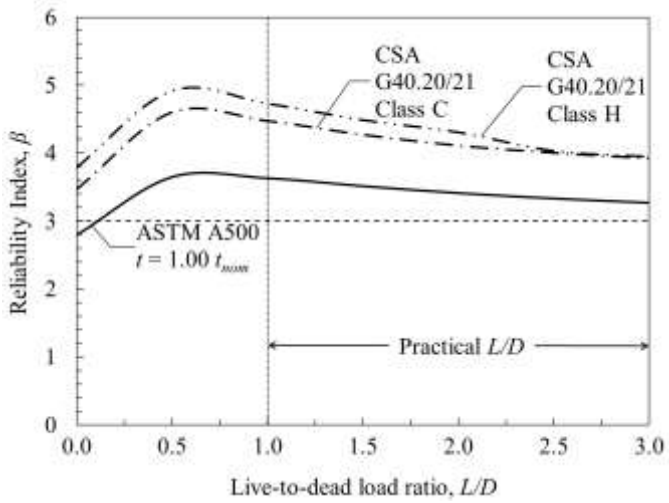

Figure 6-15: β vs. L/D ratio for CSA G40.20/21 HSS Class C and H vs. ASTM A500 CHS with $t = 1.00t_{nom}$ examined for gross section yielding

CHS under gross section yielding displays a reliability index above the target reliability index of 3.0 for all design thickness values considered. The reliability index of A500 CHS is lower than that of CSA G40 sections. This is particularly relevant to the examined case of $t = 1.00t_{nom}$, as the reliability index of the latter steel sections was only analysed at this design thickness.

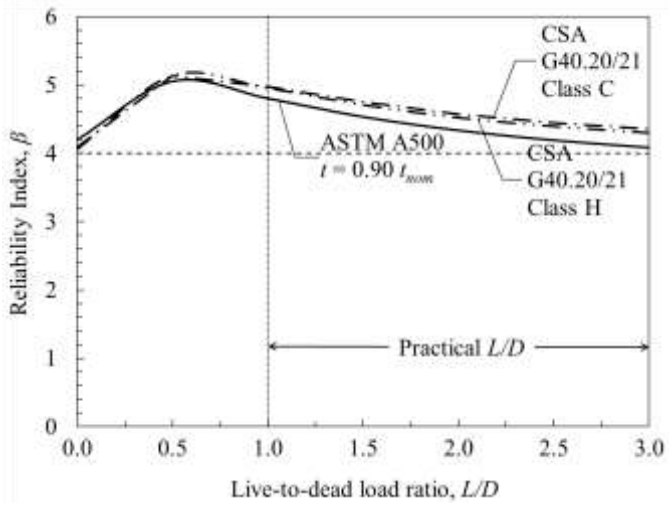

Figure 6-16: β vs. L/D ratio for CSA G40.20/21 HSS Class C and H vs. ASTM A500 CHS with $t = 0.90t_{nom}$ examined for net section fracture

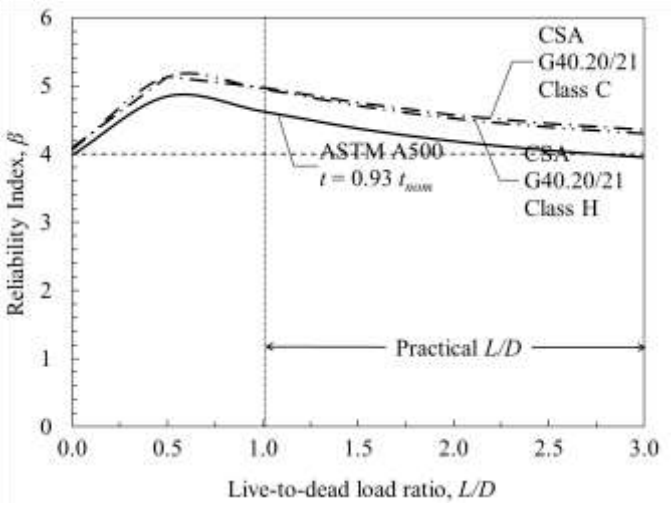

Figure 6-17: β vs. L/D ratio for CSA G40.20/21 HSS Class C and H vs. ASTM A500 CHS with $t = 0.93t_{nom}$ examined for net section fracture

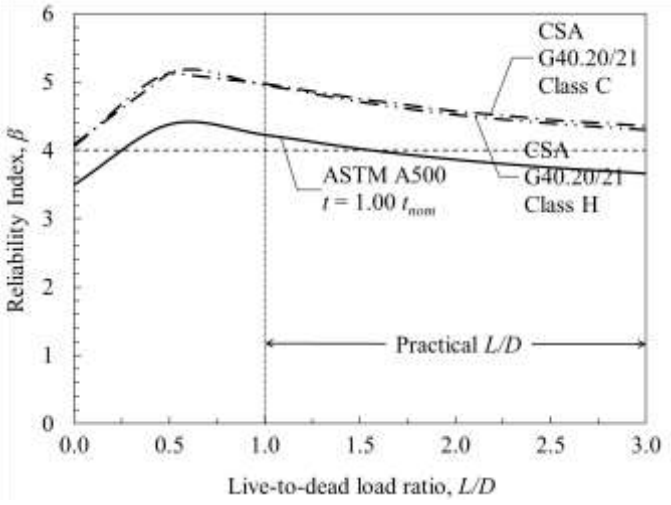

Figure 6-18: β vs. L/D ratio for CSA G40.20/21 HSS Class C and H vs. ASTM A500 CHS with $t = 1.00t_{nom}$ examined for net section fracture

For CHS analysed for axial tension failure through net section fracture for the design thickness of $0.90t_{nom}$, the reliability index was found to be above the target reliability index. When the design thickness is increased to $0.93t_{nom}$ displays a reliability index that dips below the target reliability index of 4.0 at greater values of L/D (≥ 2.75). Similar to RHS, the result can be taken as meeting the target for the purposes of common practical design considerations. For the design thickness consideration of $1.00t_{nom}$, the reliability index does not meet the target as it falls below the value of 4.0 for most of the practical load ratio range.

6.3. LATERALLY SUPPORTED BENDING MEMBERS

Figures 6-19, 6-20 and 6-21 depict the calculated β values as a function of L/D for RHS members in bending which meet Class 1 and Class 2 requirements. Figures 6-22, 6-23 and 6-24 present the same for RHS members which meet Class 3 requirements. Therein, the solid black lines represent the average β for all sections analysed, and the target $\beta = 3.0$ is indicated by a dashed horizontal line. The results of the analysis are presented side-by-side with the results of the G40.20/21 study conducted by Schmidt and Bartlett (2002), except in the case of Class 3 sections which the previous study did not consider.

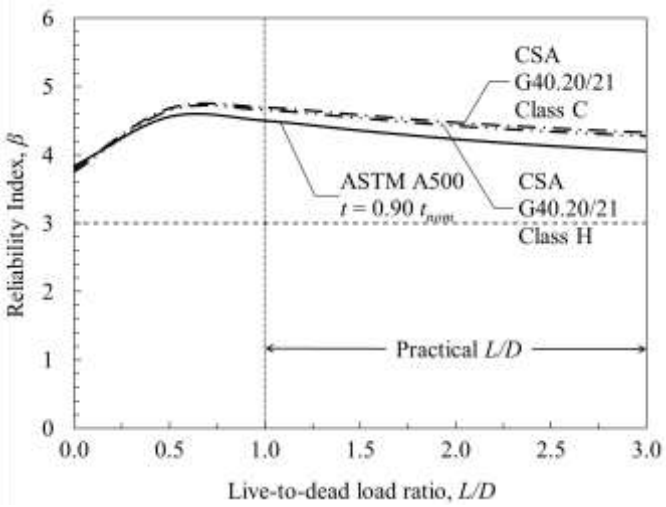

Figure 6-19: β vs. L/D ratio for CSA G40.20/21 HSS Class C and H vs. ASTM A500 Class 1 and 2 RHS with $t = 0.90t_{nom}$ examined for laterally supported bending

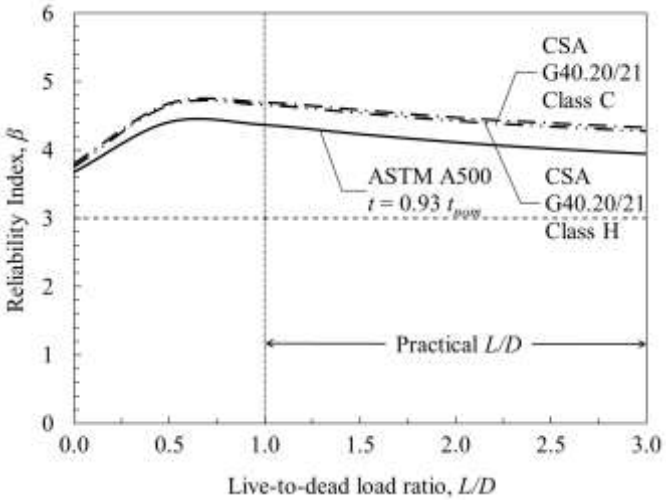

Figure 6-20: β vs. L/D ratio for CSA G40.20/21 HSS Class C and H vs. ASTM A500 Class 1 and 2 RHS with $t = 0.93t_{nom}$ examined for laterally supported bending

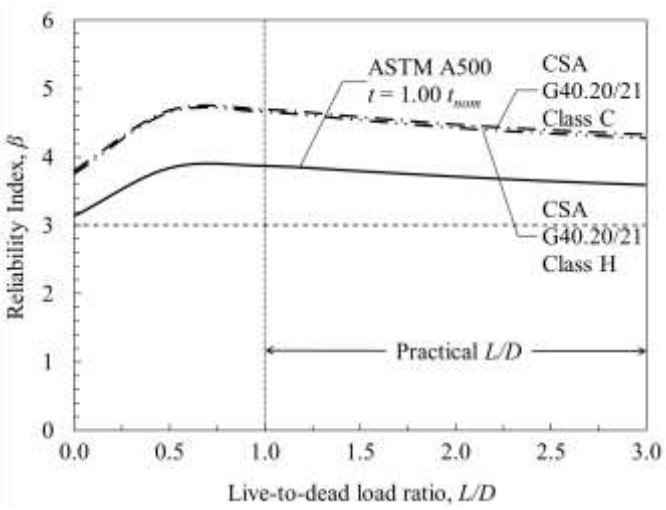

Figure 6-21: β vs. L/D ratio for CSA G40.20/21 HSS Class C and H vs. ASTM A500 Class 1 and 2 RHS with $t = 1.00t_{nom}$ examined for laterally supported bending

Class 1 and 2 RHS analysed for laterally supported bending displays a reliability index that satisfies the target reliability index of 3.0 at all values of L/D for design thickness set at $t = 0.90$, 0.93 and $1.00t_{nom}$.

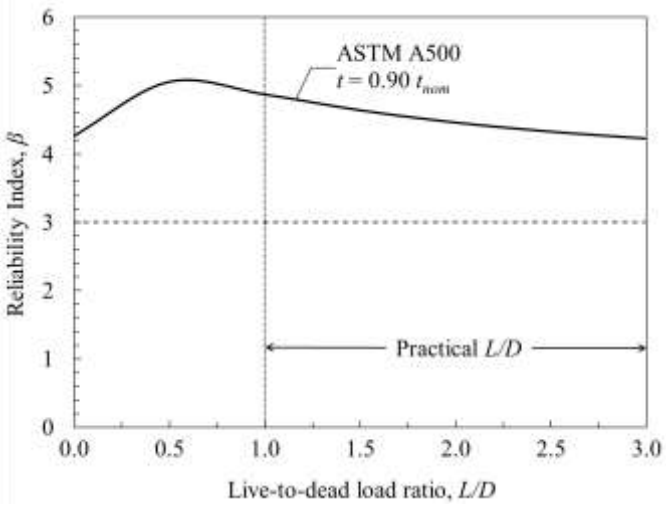

Figure 6-22: β vs. L/D ratio for ASTM A500 Class 3 RHS with $t = 0.90t_{nom}$ examined for laterally supported bending

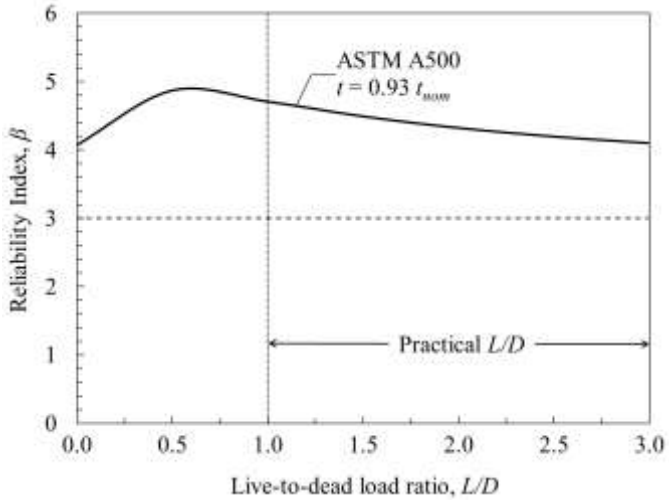

Figure 6-23: β vs. L/D ratio for ASTM A500 Class 3 RHS with $t = 0.93t_{nom}$ examined for laterally supported bending

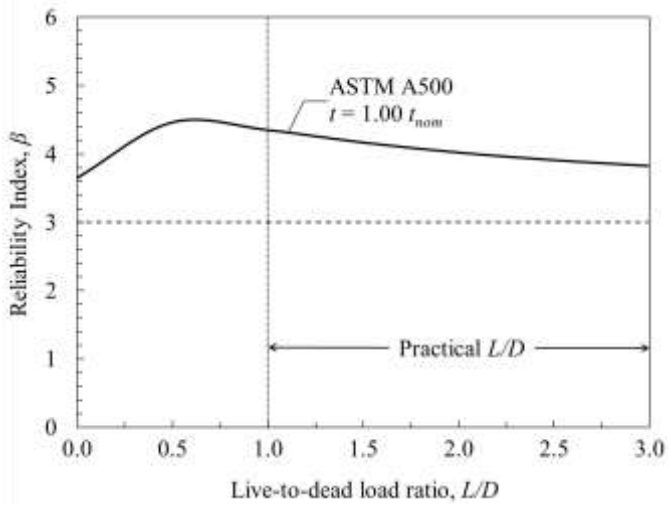

Figure 6-24: β vs. L/D ratio for ASTM A500 Class 3 RHS with $t = 1.00t_{nom}$ examined for laterally supported bending

Class 3 RHS analysed for laterally supported bending displays a reliability index that satisfies the target reliability index of 3.0 at all values of L/D for design thickness set at $t = 0.90$, 0.93 and $1.00t_{nom}$.

Figures 6-25, 6-26 and 6-27 depict the calculated β values as a function of L/D for RHS members in bending which meet Class 1 and Class 2 requirements. Therein, the solid black lines represent the average β for all sections analysed, and the target $\beta = 3.0$ is indicated by a dashed horizontal line. The results of the analysis are presented side-by-side with the results of the G40.20/21 study conducted by Schmidt and Bartlett (2002), except in the case of Class 3 sections which the previous study did not consider. The sampled data for this study did not contain any CHS sections meeting Class 3 requirements, and as such no results are available for this.

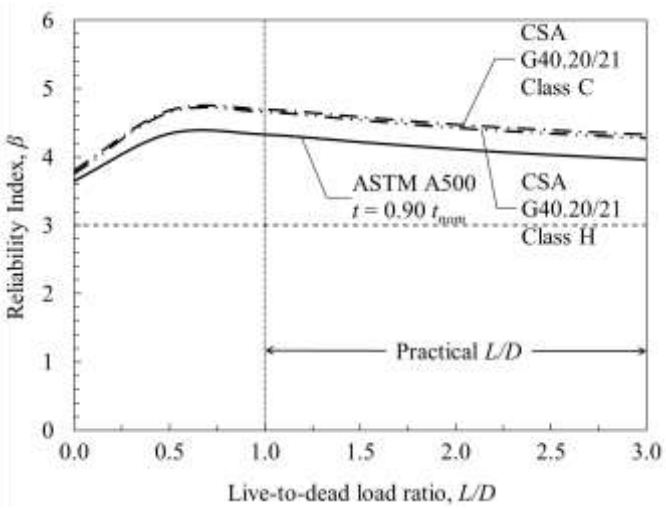

Figure 6-25: β vs. L/D ratio for CSA G40.20/21 HSS Class C and H vs. ASTM A500 Class 1 and 2 CHS with $t = 0.90t_{nom}$ examined for laterally supported bending

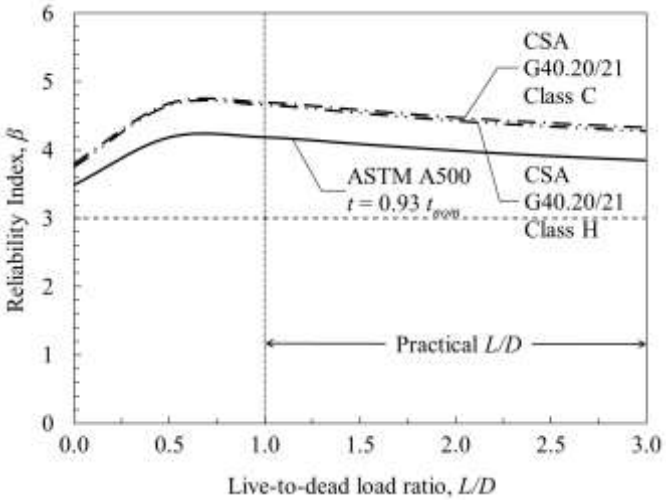

Figure 6-26: β vs. L/D ratio for CSA G40.20/21 HSS Class C and H vs. ASTM A500 Class 1 and 2 CHS with $t = 0.93t_{nom}$ examined for laterally supported bending

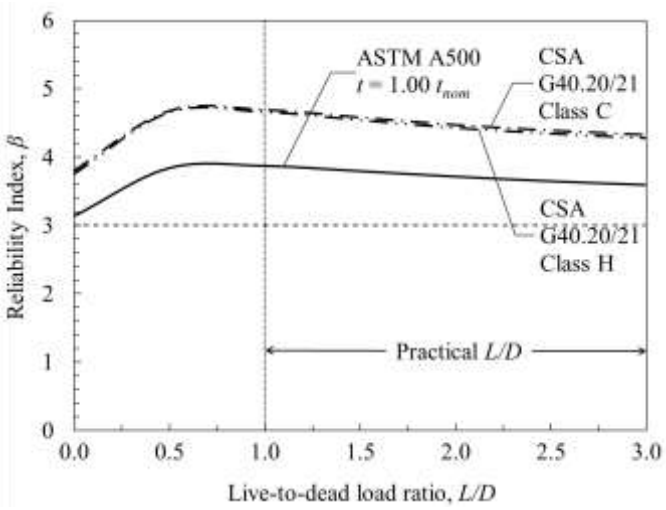

Figure 6-27: β vs. L/D ratio for CSA G40.20/21 HSS Class C and H vs. ASTM A500 Class 1 and 2 CHS with $t = 1.00t_{nom}$ examined for laterally supported bending

Class 1 and 2 CHS analysed for laterally supported bending displays a reliability index that satisfies the target reliability index of 3.0 at all values of L/D for design thickness set at $t = 0.90$, 0.93 and $1.00t_{nom}$.

FORM analysis conducted for the bending capacity specified by Clause 13 of CSA S16:24 shows that $t = 0.90$, 0.93, and $1.00t_{nom}$ all provide reliability indices (β) above the target (i.e., $\beta > 3.0$) for RHS and CHS tension members made to ASTM A500.

The current ASTM A500 design wall thickness given by CSA and the CISC ($t = 0.90t_{nom}$) is conservative for HSS members in bending. It would be justified to adopt a design wall thickness of $t = 0.93t_{nom}$ for gross section yielding to harmonize CSA S16's requirements with AISC 360, for consistency across standards. For maximum economy, a design wall thickness of $t = 1.00t_{nom}$ for A500 HSS members under bending may also be justified.

No data was available for sections meeting Class 3 requirements for CHS. The study therefore obtained no results for these. RHS sections meeting Class 3 parameters were analysed, against the bending capacity specified by Clause 13 of CSA S16:24, with the results meeting the target reliability index for all assessed values of the design wall thickness.

The current design wall thickness for RHS is conservative in bending and should be revised upwards to either $0.93t_{nom}$ for harmonization or to $1.00t_{nom}$ for maximum economy.

Chapter 7: DEFLECTION ANALYSIS

An analysis was performed to ascertain the relationship between the section thickness (actual vs. assumed) with the stiffness of the section under different support configurations. The member stiffness was calculated and normalised for the average member thickness and compared to the stiffness obtained when assuming a design thickness $t = 0.90$, 0.93 and $1.00t_{nom}$.

A 219.1 x 8 mm CHS beam was considered for the analysis. Geometric and material parameters for the section were drawn from the study. In the deflection analysis, the beam was considered as being loaded with a uniformly distributed load of magnitude W kN/m along its span of length L. When assumed to have fixed end supports, the beam stiffness, k_b is obtained from beam theory as:

$$k_b = \frac{384EI}{L^4} \tag{7-1}$$

where E and I are the modulus of elasticity and the moment of inertia respectively.

Similarly, when simple supports are assumed for the beam:

$$k_b = \frac{384EI}{5L^4} \tag{7-2}$$

and for a cantilever beam with full fixity at one end:

$$k_b = \frac{8EI}{L^4} \tag{7-3}$$

Under axial loading, the stiffness (k_a) of the considered section can be obtained from:

$$k_a = \frac{AE}{L} \tag{7-4}$$

Considering the selected CHS section and using the properties collected for this study, stiffness values were computed at different thickness values for comparison. The considered thickness values were the average section thickness ($0.921t_{nom}$), the average profile average for all CHS sections considered in this study

(0.929t_{nom}), and the design thickness values considered in this study (0.90, 093 and 1.00t_{nom}). The results are presented in table 7-1 below.

Table 7-1: Variation of section stiffness with wall thickness for a CHS 219 x 8mm

Wall thickness (x t_{nom}, mm)	Cross-sectional Area, A (x 10^3 mm^2)	Moment of Inertia, I (x 10^9 mm^4)	Axial Stiffness, k_a (x 10^3 E/L kN/mm^2)	Bending Stiffness, k_b (x 10^{11} E/L^4 kN/mm^2)		
				Simply supported	Fixed-fixed	Fixed cantilever
0.90	4.896	1.758	4.896	1.350	6.750	0.141
0.921	5.004	1.794	5.004	1.378	6.889	0.144
0.929	5.048	1.808	5.048	1.389	6.944	0.145
0.93	5.053	1.810	5.053	1.390	6.951	0.145
1.00	5.419	1.931	5.419	1.483	7.415	0.154

The results of the analysis indicate that there is minimal variation in the member stiffness under all load conditions when the thickness is varied between the average profile thickness (0.929t_{nom}) and the assumed value of the design thickness at 0.93t_{nom}.

The assumed thickness of 0.93t_{nom} gives a stiffness nearly equal to the average measured profile thickness for CHS (i.e., not more than 0.1% difference in any case), indicating that deflection estimates would not be adversely affected by a new design wall thickness in both bending and pure axial loading. The results for the higher assumption, such as 1.00t_{nom} indicates larger deviation from the mean (i.e., up to 6.8%, in the worst case), and as such the accuracy of deflection predictions may be unacceptable at this higher level.

A similar analysis was completed using an RHS 305 x 305 x 7.9 mm, yielding similar results (see Table 7-2 below).

Table 7-2: Variation of section stiffness with wall thickness for a RHS 305 x 305 x 7.9 mm

Wall thickness (x t_{nom}, mm)	Cross-sectional Area, A (x 10^3 mm^2)	Moment of Inertia, I (x 10^9 mm^4)	Axial Stiffness, k_a (x 10^3 E/L kN/mm^2)	Bending Stiffness, k_b (x 10^{11} E/L^4 kN/mm^2)		
				Simply supported	Fixed-fixed	Fixed cantilever
0.90	8.387	1.398	8.387	1.074	5.370	0.112
0.911	8.486	1.414	8.486	1.086	5.429	0.113
0.924	8.602	1.432	8.602	1.100	5.499	0.114
0.93	8.655	1.440	8.655	1.106	5.531	0.115
1.00	9.278	1.538	9.278	1.181	5.904	0.123

Chapter 8: SUMMARY, CONCLUSIONS AND RECOMMENDATIONS

8.1. SUMMARY

The production of ASTM A500 structural steel products is governed by ASTM A500/A500M-23, which allows for a permissible deviation in the wall thickness of HSS products of -10%. No tolerance limits are set by the standard for mass weight and cross-sectional area.

The design of A500 HSS is guided by CSA and CISC through the CSA S16:24 design standard, applicable to all design work in Canada. The design code specifies a design wall thickness of 90% of the nominal wall thickness of the section, i.e, $t = 0.90t_{nom}$. Design of A500 HSS in the United States of America is guided by the AISC through AISC 360-16, which stipulates a higher design thickness of $0.93t_{nom}$. This gives rise to questions as to the economy of the Canadian standard, especially given recent changes in manufacturing standards of A500 HSS:

i. The minimum yield strength for ASTM Grades B and C HSS has been harmonised to 315 MPa and 345 MPa, respectively.
ii. The measured material properties routinely exceed the minimum specified yield strength, as noted by Liu (2016).
iii. Recently introduced jumbo sections tend to meet boundary classification conditions, such that they would be used uneconomically in design.

Jumbo HSS is also becoming a more popular substitute for bulkier steel sections, finding use particularly as compression and bending resisting elements. This leads to an ever-increasing market share for HSS products, and more-so ASTM A500 products as they are the most common and popular type of structural steel in North America.

With this backdrop, the impact of the "ASTM A500 design thickness issue" has potentially sizeable and undue economic implications. These implications extend also to the environmental impact posed by structural steel. This research comes at a time when the steel production and construction industries are seeking to reduce their carbon footprint.

This study sought to review the design wall thickness requirements imposed by CSA S16:24 on ASTM A500 HSS in Canada. A large-scale sampling study was conducted to obtain dimensional data on A500 HSS production. This data was mainly drawn from producer quality control records and literature representing modern manufacturing practices. The dataset developed for this study draws on 9833 geometric measurements and forms the largest sample study of its kind. The data represents approximately 85% of the current North American market, with two steel corporations operating a total of 25 production plants across the North American continent represented.

Additional data on HSS material properties and professional factors was drawn from literature sources. A total of 53097 data points on material properties were drawn from a study by Liu (2016) and adjusted for recent revisions to the specified strength parameters for ASTM A500 HSS.

Professional factor statistics for bending were drawn from the landmark study of Kennedy and Gad Aly (1980). For gross section yielding under tension, the study conducted by Ellingwood et al. (1980) provided the professional factor statistics, while the same for net section fracture were obtained from Gagnon and Kennedy (1989). The compression professional factor statistics were drawn from the work of Bjorhovde and Birkemoe (1979).

The dimensional and material data obtained were used to compute relevant statistical parameters for carrying out a First Order Reliability Method (FORM) analysis of the inherent reliability of the member resistance specified in Clause 13 of CSA S16:24 (CSA 2024). Member resistance under axial tension, axial compression and laterally supported bending were considered. In all the analysis conditions, the design wall thickness was analysed at 0.90, 0.93 and 1.00t_{nom}.

The safety index was calculated over the range of live-to-dead load ratios between 0 and 3, i.e. $0 \leq L/D \leq 3$. The safety index is a measure of the margin of safety against failure. This was compared, over the practical live-to-dead load ratio range from 1 to 3, against target reliability indices specified by CSA S408-11 (CSA 2011). The target reliability index of 4.0 is applied to brittle failure modes, while the lower target of 3.0 is applied to ductile failure. The higher safety index for brittle failure reflects their sudden and catastrophic nature, unlike ductile failures which can often be noticed and remediated before total structural failure occurs.

From the load and resistance statistics developed, a FORM analysis was conducted, and the results compared to similar studies on CSA G40.20/21 HSS for validation of the analysis.

The results obtained generally indicate that the design specifications of CSA S16:24 (CSA 2024) with respect to the design wall thickness are over-conservative. This is particularly evident in axial compression, axial tension under gross section yielding and in laterally supported bending. In these cases, the safety index is above the target reliability index for design wall thicknesses up to and including t_{nom}.

Axial tension under net section fracture analyses fell below the target reliability index at extreme values of L/D. The results can be taken to meet the target for common design considerations, as the high L/D range is atypical for common design consideration.

8.2. CONCLUSIONS

8.2.1. COMPRESSION MEMBERS

FORM analysis over the practical range of live-to-dead *(L/D)* load ratios ($1 \leq L/D \leq 3$) against the axial compressive resistance specified by Clause 13.1.1.1 of CSA S16:24 (CSA 2024) shows that $t = 0.90$, 0.93, and $1.00t_{nom}$ all provide reliability indices (β) above the target (i.e., $\beta > 3.0$) for RHS and CHS compression members made to ASTM A500.

The current ASTM A500 design wall thickness given by CSA and the CISC ($t = 0.90t_{nom}$) is conservative for HSS members in compression. It would be justified to adopt a design wall thickness of $t = 0.93t_{nom}$ in compression to harmonize CSA S16's requirements with AISC 360, for consistency across standards. For maximum economy, a design wall thickness of $t = 1.00t_{nom}$ for A500 HSS compression members may also be justified.

8.2.2. TENSION MEMBERS

For tension members designed according to Clause 13.2 of CSA S16:24, the reliability analysis undertaken as part of this study showed that the design wall thickness specified is over-conservative and should be revised upward when designing A500 members for gross section yielding.

The results of the analysis at the specified design thickness when considering net section fracture fell marginally below the target reliability index when RHS is considered. This is the case at high *L/D*, a condition which is uncommon in typical design conditions. As a result, the analysis results can be taken as meeting the target for most typical load conditions. At a design thickness of $0.93t_{nom}$ for RHS, the analysis results show that the reliability index falls below the target, though this again is acceptable as the target is not met only at high L/D conditions which are uncommon in typical design considerations.

For CHS under net section fracture, the analysis results for both 0.90 and $0.93t_{nom}$ met the target reliability index specified for this failure condition. Based on the analysis results, the specified design thickness in net section fracture should be revised upwards to $0.93t_{nom}$ for improved economy in design.

8.2.3. LATERALLY SUPPORTED BENDING MEMBERS

The specified design wall thickness for laterally supported bending members designed to Clause 13.5 of CSA S16:24 is over-conservative and should be revised upwards to $0.93t_{nom}$ for design specification homogeneity in North America. A higher design wall thickness of up to $1.00t_{nom}$ may also be adopted if maximum economy is sought. This applies to both Class 1,2 and Class 3 RHS sections.

For CHS sections, the above conclusions were found adequate for sections meeting Class 1 and 2 specifications. No data was obtained for Class 3 members in this study; hence, no conclusions could be drawn.

8.2.4. DEFLECTION

Using sampled sections from the study, the impact of varying the thickness on the deflection of a member was investigated. The results of the analysis indicate that there is minimal variation in the member stiffness under all load conditions when the thickness is varied between the average profile thickness ($0.929t_{nom}$ for CHS and $0.924t_{nom}$ for RHS) and the assumed value of the design thickness at $0.93t_{nom}$. The assumed thickness of $0.93t_{nom}$ gives a stiffness nearly equal to the average measured profile thickness for both profiles (i.e., not more than 0.1% difference in any case), indicating that deflection estimates would not be adversely affected by a new design wall thickness in both bending and pure axial loading. This indicates that the proposed design thickness of $0.93t_{nom}$ provides adequate reliability across all load actions at ULS and SLS conditions considered in this study.

8.3. RECOMMENDATIONS FOR FUTURE WORK

The scope of this study was limited to axial compression, axial tension and laterally supported members. Further investigation may be warranted for:

i. laterally unsupported members where failure by lateral torsional buckling may govern (however, these are quite uncommon for HSS, and restricted to only a subset of RHS sections with high aspect ratios when bent about their major axis);
ii. members under combined bending and axial tension or compression (or beam-columns); and
iii. connections.

Additionally, no data was available for the analysis of the Class 3 CHS members in bending. Future research investigating the safety index for this sub-category may be considered necessary.

REFERENCES

AISC (2016): AISC 360-16. *Specification for structural steel buildings.* Chicago, IL, USA.

AISC (2017): *Steel construction manual*, 15th Edition. Chicago, IL, USA.

Allen, A.O., (1991): *Probability, Statistics, and Queueing Theory with Computer Science Applications*. 2nd Ed., Academic Press Professional, Inc., San Diego, CA.

Allen, D.E., (1975): *Limit States Design—A Probabilistic Study.* Canadian Journal of Civil Engineering, Vol. 2, No. 1.

Ang, A.H.S., & Cornell, C.A. (1974): *Reliability Bases of Structural Safety and Design.* Journal of the Structural Division, ASCE, Vol. 100, No. ST9, pp. 1,755–1,769.

ASTM (2015): ASTM A1085/A1085M-15. *Standard Specification for Cold-Formed Welded Carbon Steel Hollow Structural Sections (HSS).* West Conshohocken, PA, USA: American Society for Testing and Materials International.

ASTM (2020): ASTM A500/A500M-20. *Standard Specification for Cold-Formed Welded and Seamless Carbon Steel Structural Tubing in Rounds and Shapes.* West Conshohocken, PA, USA.

ASTM (2023): ASTM A500/A500M-23. *Standard specification for cold-formed welded and seamless carbon steel structural tubing in rounds and shapes.* West Conshohocken, PA, USA.

Atlas Tube (2021): *New! Atlas tube jumbo HSS [brochure]*. Atlas Tube, Chicago, IL, USA.

Barker, R., Duncan, J., Rojiani, K., Ooi, P.S.K., Tan, C. K., & Kim, S.G., (1991): *Manuals for the design of bridge foundations.* National Cooperative Highway Research Program (NCHRP) Report 343. Washington, DC: Transportation Research Board, National Research Council.

Bjorhovde, R. & Birkemoe, P.C. (1979): *Limit states design of HSS columns.* Canadian Journal of Civil Engineering, 6(2).

BSI (2006): BS EN 10219 Part 1 & 2: 2006. *Cold formed Welded Structural Sections of Non-Alloy and Fine Grain Steels.* London, United Kingdom: British Standards Institution.

BSI (2006): BS EN 10210 Part 1: 2006. *Mechanical Properties for Hot Finished Circular Hollow Sections.* London, United Kingdom: British Standards Institution.

CISC (2021): *Handbook of Steel Construction* (12th ed.). Toronto, ON, Canada: Canadian Institute of Steel Construction.

Cornell, C.A., (1969): *A Probability-based Structural Code*. Journal, American Concrete Institute, Vol. 66, No. 12.

Canadian Commission on Building and Fire Codes (2022): *National Building Code of Canada.* National Research Council of Canada.

CSA (1969): CSA S16-1969. *Steel Structures for Buildings.* Canadian Standards Association, Toronto, ON.

CSA (1974): CAN/CSA S16.1-1974. *Steel structures for buildings – limit states design.* Toronto, Canada.

CSA. (2011): CSA S408-11. *Guidelines for the development of limit states design standards.* Mississauga, ON, Canada: Canadian Standards Assocaition.

CSA. (2018): CSA G40.20-13/G40.21-13 (R2018). *General Requirements for Rolled or Welded Structural Quality Steel / Structural Quality Steel.* Toronto, ON, Canada: Canadian Standards Association.

CSA. (2024): CSA S16:24. *Design of steel structures*. Toronto, Canada (2024).

European Committee for Standardization (2006): EN 10219-2:2006 *Cold-formed welded structural hollow sections of non-alloy and fine grain steels - Part 2: Tolerances, dimensions, and sectional properties.* CEN - European Committee for Standardization. Brussels, Belgium.

Ellingwood, B., Galambos, T., MacGregor, J., Cornell, C. (1980): *Development of probability-based load criterion for American national standard A58.* Special Publication 577.

Fisher, J.W., Galambos, T.V., Kulak, G.L., & Ravindra, M.K. (1978), *Load and resistance factor design criteria for connectors.* Journal of the Structural Division, ASCE, Vol. 104, No. 9, pp. 1,427–1,441.

Foley, C.M., Marquez, A. (2011): *Characterizing dimensional variability in HSS members.* American Institute of Steel Construction. Chicago, Illinois, USA.

Gagnon, D.P. and Kennedy, D.J.L. (1989): *Behavior and Ultimate Tensile Strength of Partial Joint Penetration Groove Welds.* Canadian Journal of Civil Engineering, Vol. 16.

Galambos, T.V., & Ravindra, M.K. (1973): *Tentative load and resistance factor design criteria for steel buildings.* Research Report No. 18, Civil Engineering Department, Washington University, St. Louis, MO.

Galambos, T.V., & Ravindra, M.K. (1977): *The basis for load and resistance factor design criteria of steel building structures.* Canadian Journal of Civil Engineering, 4(2):178-189.

Galambos, T.V., & Ravindra, M.K. (1978): *Load and resistance factor design for steel.* Journal of the Structural Divisions, 104(9), 1337-1353.

Galambos, T., & Ravindra, M. (1981): *Load and resistance factor design*. Engineering Journal, AISC, 18(3), 78 – 84.

Jollymore, I.M., Tousignant, K., & Packer, J.A. (2024). *Review and Evaluation of the Separation Factor Approach for Structural Reliability.*

Kariyawasam, S.N., Rogowsky, D.M., & MacGregor, J.G., (1997): *Resistance factors and companion-action load factors for reinforced concrete building design in Canada.* Canadian Journal of Civil Engineering 24(4).

Kennedy, D., Baker, K. (1984): *Resistance Factors for Steel Highway Bridges*. Canadian Journal of Civil Engineering, 11, 324-334.

Kennedy, D., & Gad Aly, M. (1980). *Limit state design of steel structures - performance factors.* Canadian Journal of Civil Engineering, 7: 45-77.

Kulak, G.L., & Grondin, G.Y. (2021): *Limit states design in structural steel.* 11th edition. Canadian Institute of Steel Construction.

Lind, N.C., (1971): *Consistent Partial Safety Factors.* Journal of the Structural Division, ASCE, Vol. 97, No. ST6, pp. 1,651–1,669.

Liu, J. (2016): *Updates to expected yield stress and tensile strength ratios for determination of expected member capacity in the 2016 AISC Seismic Provisions.* Engineering Journal, 2016(4), 215-228.

Nowak, A.S., & Lind, N.C., (1979): *Practical code calibration procedures.* Canadian Journal of Civil Engineering 6(1).

Nucor Corporation (2023): *Nucor Corporation Annual Report*. https://nucor.gcs-web.com/static-files/8b88e651-db97-460a-803b-7df2f01b3451, last accessed 05 October 2023.

SABS. (2011). *Steel Tubes for Non-Pressure Purposes. SANS 657-1:2011.* Pretoria, South Africa: South African Bureau of Standards.

Schmidt, B.J. (2000): *Review of the resistance factor for steel*. Digitized Theses. 3771 (2000). https://ir.lib.uwo.ca/digitizedtheses/3771.

Schmidt, B., & Bartlett, F. (2002a). *Review of Resistance Factor for Steel: Data Collection.* Canadian Journal of Civil Engineering, 29, 98-108.

Schmidt, B., & Bartlett, F. (2002b). *Review of Resistance Factor for Steel: Resistance Distributions and Resistance Factor Calibration.* Canadian Journal of Civil Engineering, 29, 109-118.

Standards Australia (2016). *Cold-Formed Structural Steel Hollow Sections. AS/NZS 1163:2016.* Sydney, Australia: Standards Australia.

STI. (2021). *Methods to Check Dimensional Tolerances on Hollow Structural Sections*. Chicago, IL, USA: Steel Tube Institute.

Thoft-Christensen, P., & Baker, M.J., (1982): *Structural Reliability Theory and Its Applications.* Springer-Verlag, New York, N.Y.

Zekelman Industries (2023): *Zekelman Industries Company Information.* https://www.zekelman.com/wp-content/uploads/2021/09/Zekelman-IndustriesCompany-Information.pdf, last accessed 05 October 2023.

Ziemian, R.D. (2010): *Guide to Stability Design Criteria for Metal Structures:* Sixth Edition. 10.1002/9780470549087.

Appendix A: PROFESSIONAL FACTORS

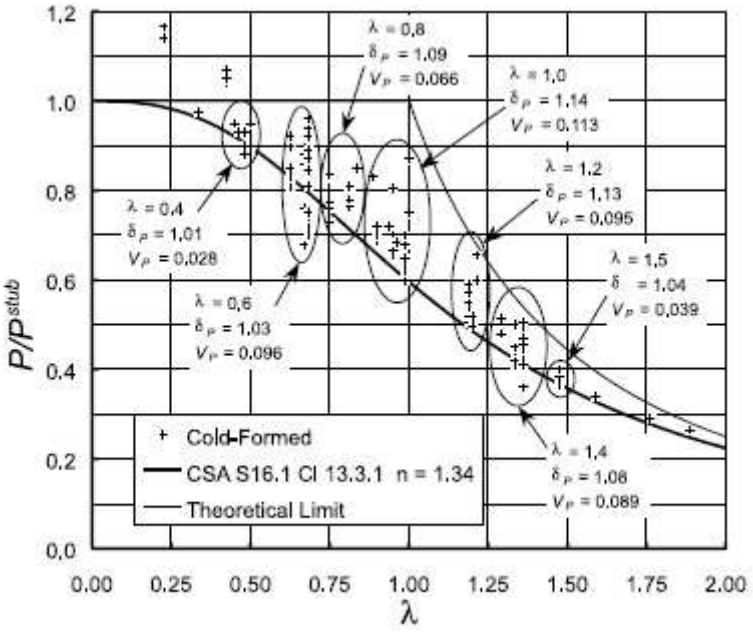

Figure A-1: Statistical parameters of professional factors for Class C HSS (Bjorhovde and Birkemoe, 1979)

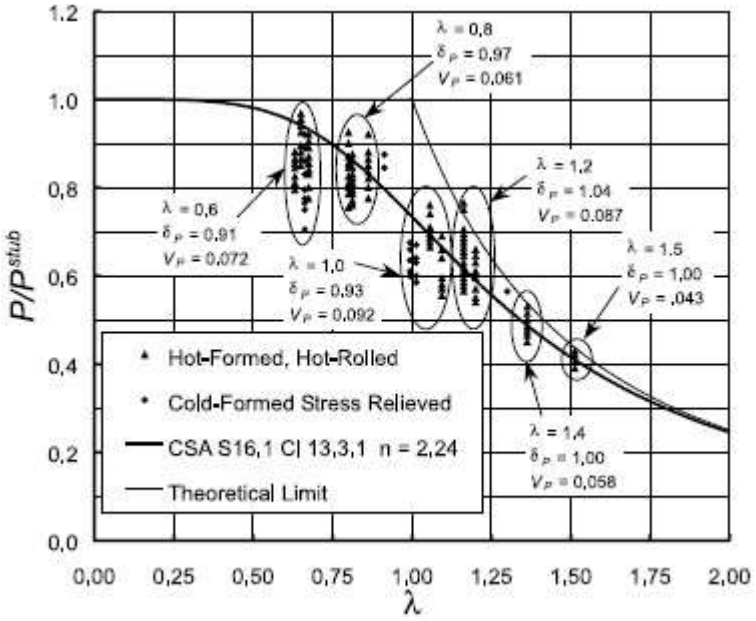

Figure A-2: Statistical parameters of professional factors for Class H HSS (Bjorhovde and Birkemoe, 1979)

Appendix B: VARIATION OF THICKNESS BIAS COEFFICIENT

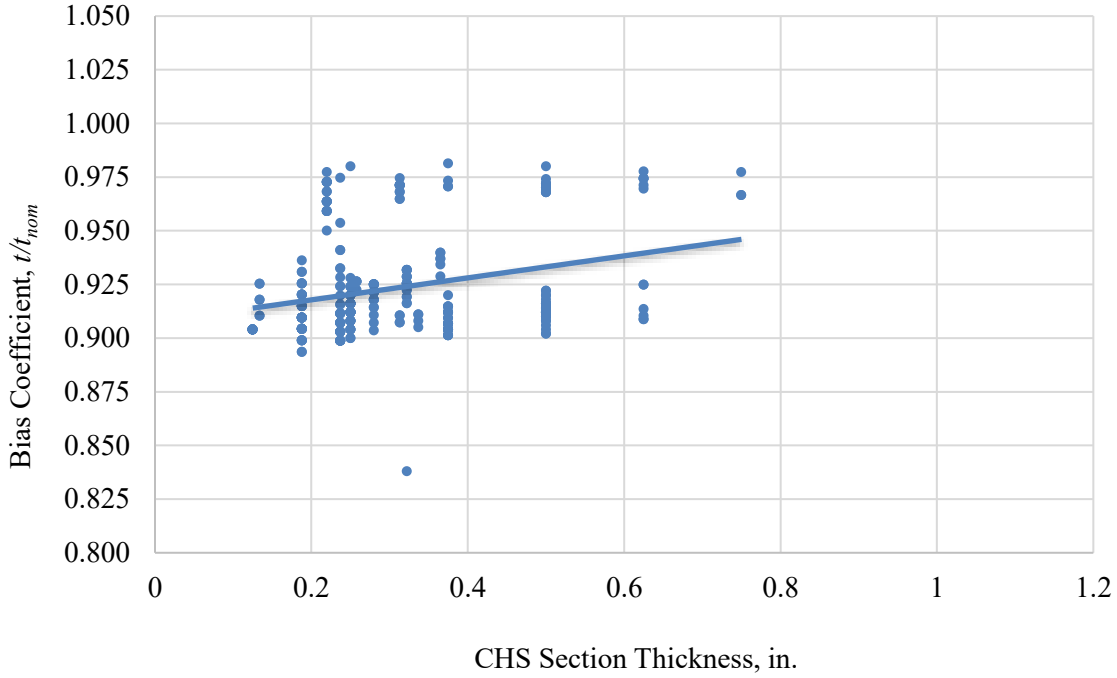

Figure B-3: Variation of thickness bias coefficient with CHS section thickness

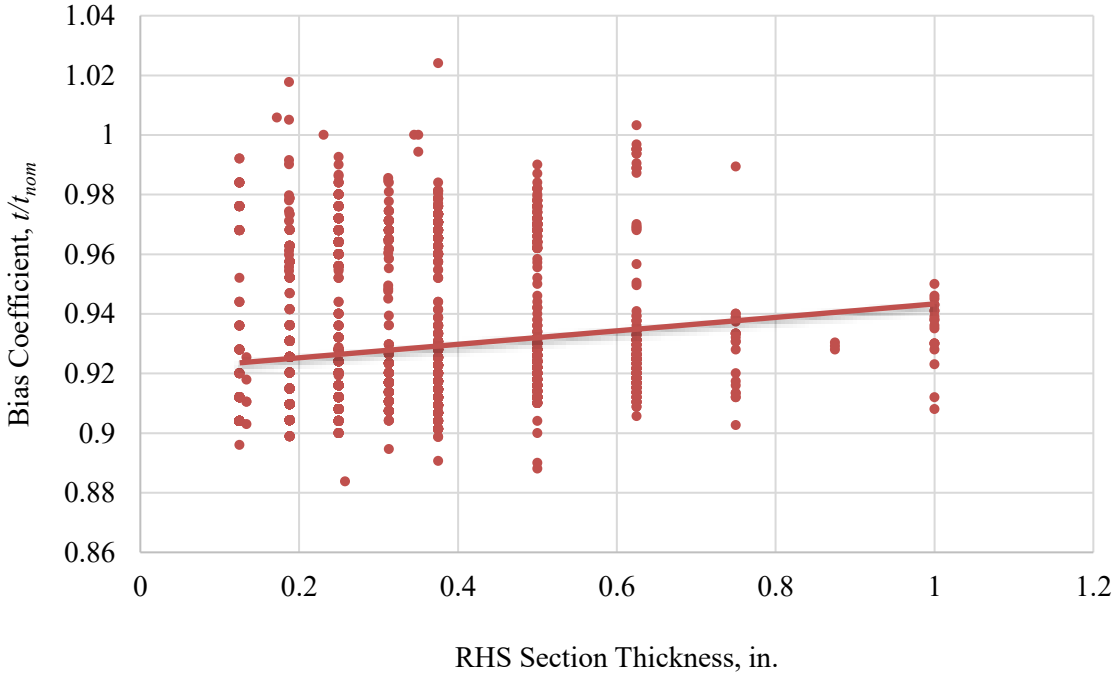

Figure B-4: Variation of thickness bias coefficient with RHS section thickness

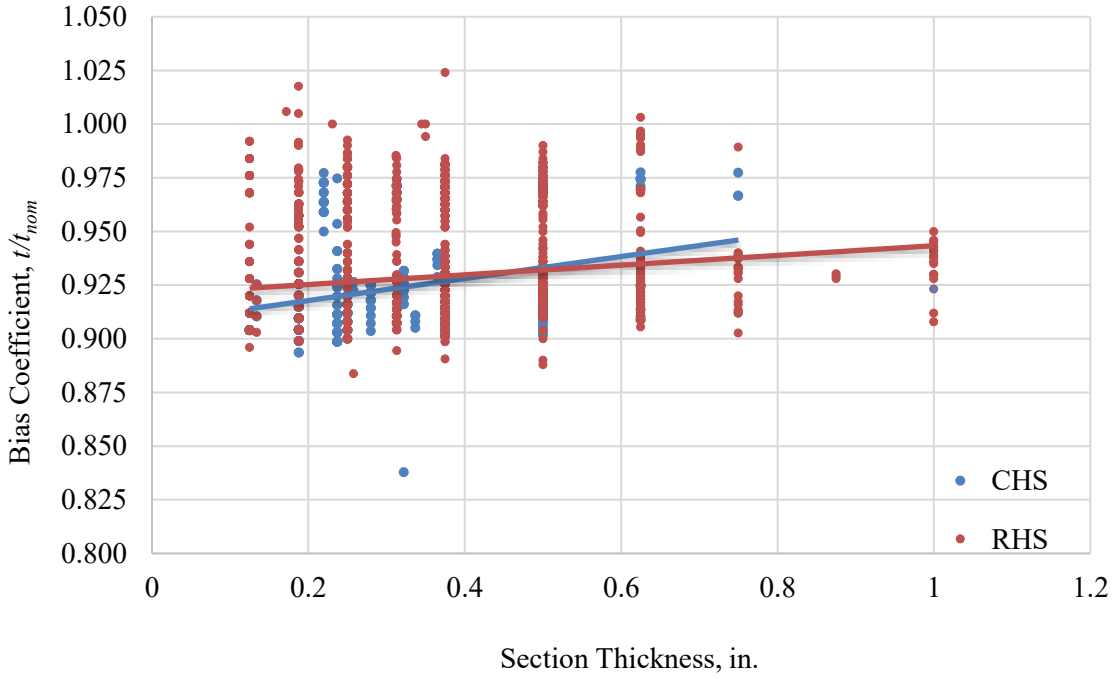

Figure B-5: Comparison of bias coefficient for CHS and RHS

Appendix C: THICKNESS VARIATIONS

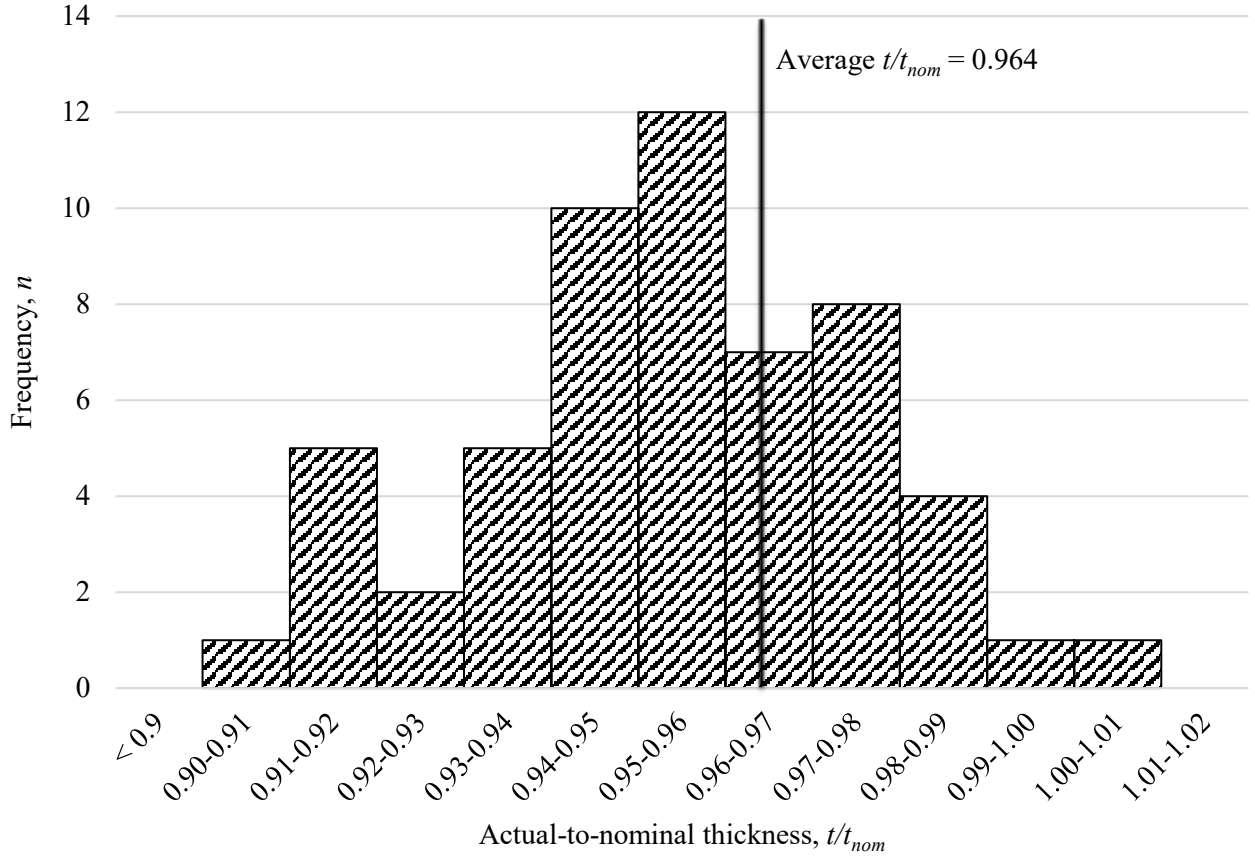

Figure C-6: Frequency vs. actual-to-nominal thickness t/t_{nom} for AISC (2011) measurements

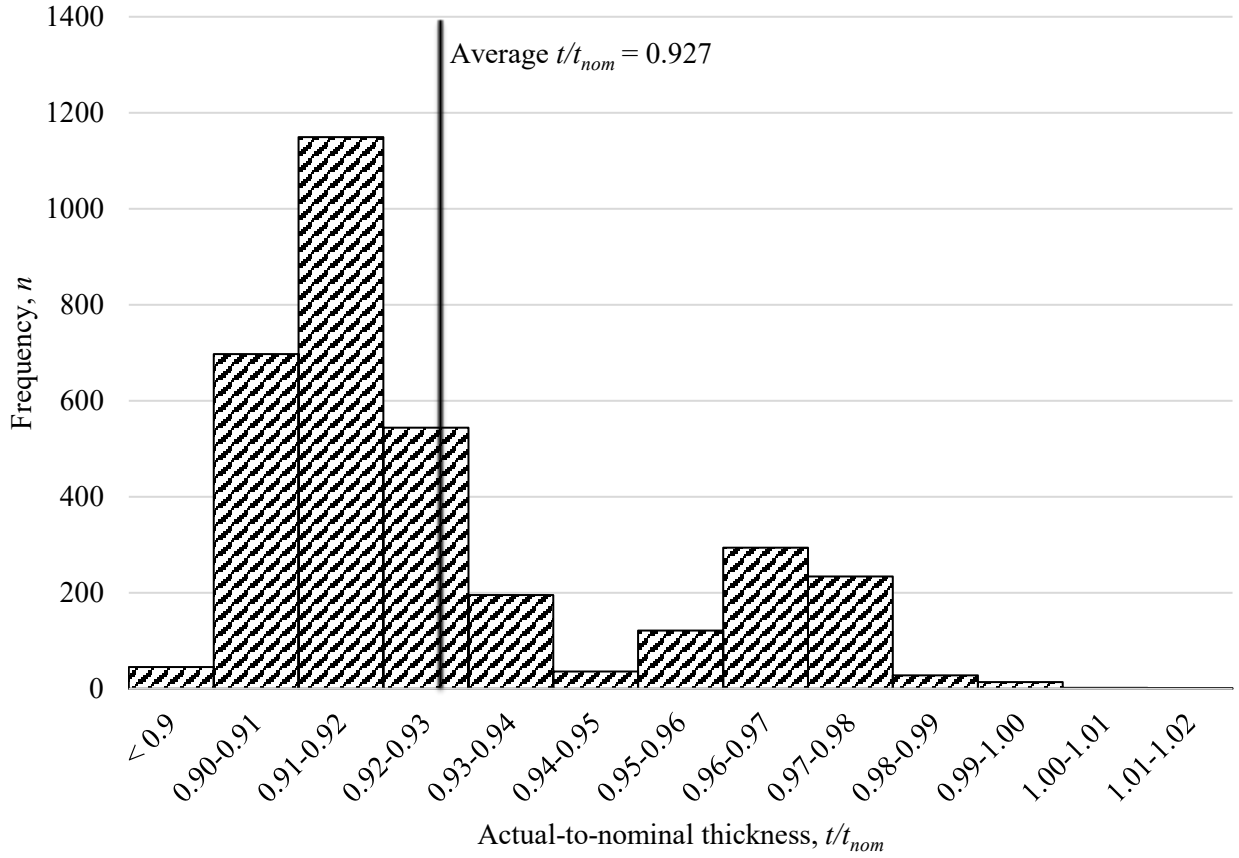

Figure C-7: Frequency vs. actual-to-nominal thickness t/t_{nom} for Producer A measurements

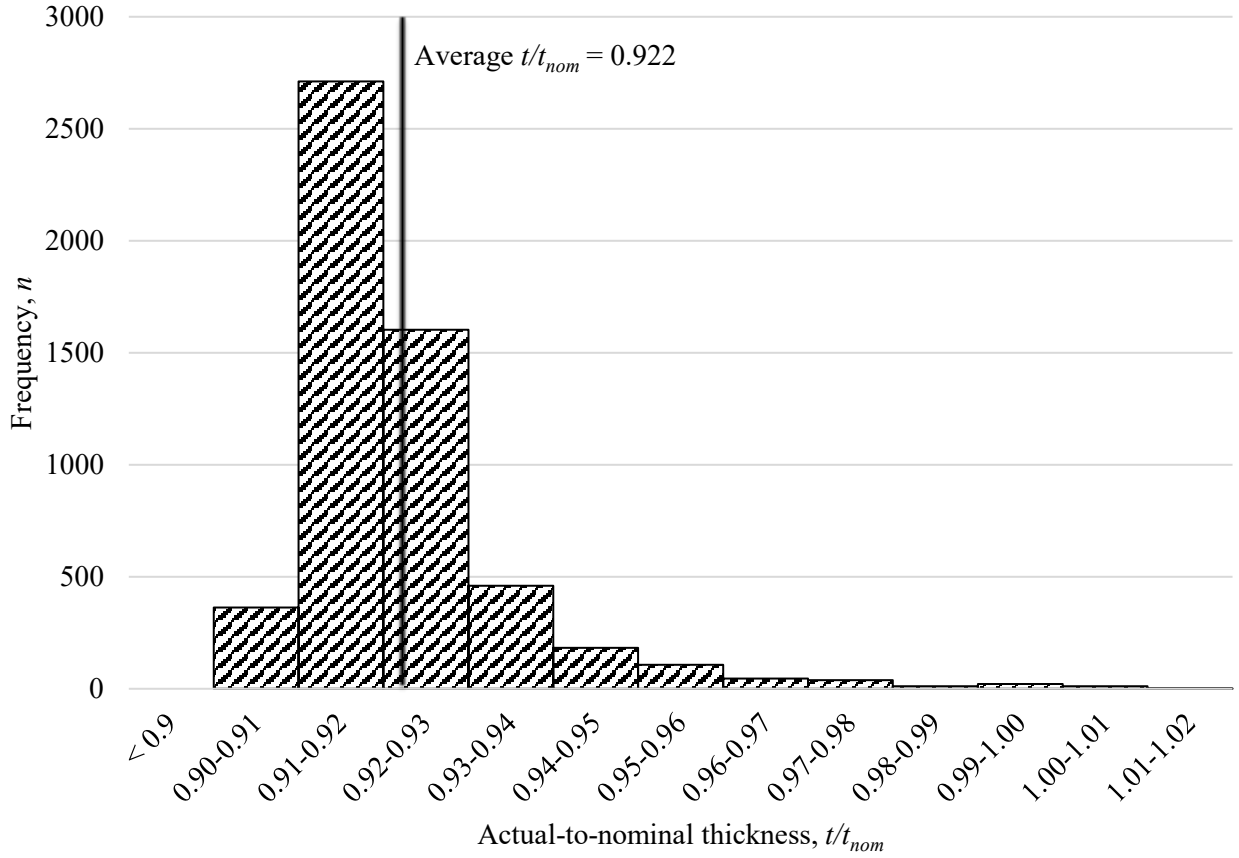

Figure C-8: Frequency vs. actual-to-nominal thickness t/t_{nom} for Producer B measurements